minerals

MDPI

Article

Electron Donor Utilization and Secondary Mineral Formation during the Bioreduction of Lepidocrocite by *Shewanella putrefaciens* CN32

Edward J. O'Loughlin [1,*], Christopher A. Gorski [2,3], Theodore M. Flynn [1,4] and Michelle M. Scherer [2]

1 Biosciences Division, Argonne National Laboratory, Lemont, IL 60439-4843, USA
2 Department of Civil and Environmental Engineering, University of Iowa, Iowa City, IA 52242-1527, USA
3 Department of Civil and Environmental Engineering, The Pennsylvania State University, University Park, PA 16802-7304, USA
4 California Department of Water Resources, 3500 Industrial Blvd, West Sacramento, CA 96691, USA
* Correspondence: oloughlin@anl.gov; Tel.: +1-630-252-9902

Received: 30 April 2019; Accepted: 4 July 2019; Published: 14 July 2019

Abstract: The bioreduction of Fe(III) oxides by dissimilatory iron reducing bacteria (DIRB) may result in the production of a suite of Fe(II)-bearing secondary minerals, including magnetite, siderite, vivianite, green rusts, and chukanovite; the formation of specific phases controlled by the interaction of various physiological and geochemical factors. In an effort to better understand the effects of individual electron donors on the formation of specific Fe(II)-bearing secondary minerals, we examined the effects of a series of potential electron donors on the bioreduction of lepidocrocite (γ-FeOOH) by *Shewanella putrefaciens* CN32. Biomineralization products were identified by X-ray diffraction, Mössbauer spectroscopy, and scanning electron microscopy. Acetate, citrate, ethanol, glucose, glutamate, glycerol, malate, and succinate were not effectively utilized for the bioreduction of lepidocrocite by *S. putrefaciens* CN32; however, substantial Fe(II) production was observed when formate, lactate, H_2, pyruvate, serine, or N acetylglucosamine (NAG) was provided as an electron donor. Carbonate or sulfate green rust was the dominant Fe(II)-bearing secondary mineral when formate, H_2, lactate, or NAG was provided, however, siderite formed with pyruvate or serine. Geochemical modeling indicated that pH and carbonate concentration are the key factors determining the prevalence of carbonate green rust verses siderite.

Keywords: green rust; siderite; dissimilatory iron reduction; iron oxide

1. Introduction

Iron (Fe) is a highly abundant element in the lithosphere. Fe-bearing clay minerals (smectites, illites, chlorites, etc.) and Fe oxides (including formal Fe oxides, oxyhydroxides, and hydroxides such as ferrihydrite, hematite (α-Fe_2O_3), maghemite (γ-Fe_2O_3), magnetite (Fe_3O_4), goethite (α-FeOOH), and lepidocrocite (γ-FeOOH)) are common constituents of soils and sediments. The biogeochemistry of Fe in most aquatic and terrestrial environments is driven largely by microbial activity, particularly in Fe-rich soils and sediments where Fe redox cycling by microorganisms is a significant component of C cycling and energy flux [1–5]. As such, the presence of Fe(II) in suboxic to anoxic near surface environments is typically the result of the activity of dissimilatory iron-reducing (DIR) bacteria and archaea. These phylogenetically diverse microorganisms can couple the oxidation of organic compounds or hydrogen (H_2) to the reduction of Fe(III) to Fe(II) [6–19]. As a group, dissimilatory iron-reducing bacteria (DIRB) are able to use soluble Fe(III) complexes (e.g., ferric citrate), Fe(III) oxides, and Fe(III)-bearing clay minerals as terminal electron acceptors for anaerobic respiration [20–28].

Living biomass aside, the pool of natural organic matter (NOM) in typical surface and near-subsurface environments is comprised primarily of low-molecular-mass components (<1 kDa) that usually include fatty acids and free sugars and amino acids, along with high-molecular-mass (>1 kDa) components that consist largely of humic substances, with lesser amounts of proteins, carbohydrates, and other non-humic macromolecules [29]. The pool of NOM is highly dynamic, largely due to microbial activity. Under anoxic conditions, complex NOM (e.g., proteins, carbohydrates, and lipids) are depolymerized by hydrolytic enzymes from a broad range of microorganisms [30] and the hydrolysis products (e.g., amino acids, monosaccharide, and fatty acids), serve as substrates for fermentation. In turn, fermentative microorganisms produce a suite of fatty acids (formate, acetate, lactate), alcohols (ethanol, butanol), and H_2, which can be utilized as electron donors for anaerobic respiration by a broad range of facultative and obligate anaerobes including DIRB [31].

The products of DIR comprise a broad range of Fe(II) species including soluble and adsorbed Fe(II) and mineral phases containing structural Fe(II) (e.g., magnetite, siderite ($FeCO_3$), vivianite [$Fe_3(PO_4)_2{\cdot}8H_2O$], green rust, chukanovite [$Fe_2(OH)_2CO_3$], and Fe(II)-bearing clays) [32–40]. Many factors have been identified as contributing to the formation of specific Fe(II)-bearing secondary minerals as products of DIR, including Fe(III) oxide mineralogy, [20,35]; Fe(III) oxide particle aggregation, [41]; the rate and extent of Fe(II) production, [33,35,42,43]; the presence of electron shuttles, [33]; the species and population size of the DIRB, [44–46]; the presence of oxyanions (phosphate, silicate, molybdate, arsenate, etc.), [33,44,47–49]; the type/nature of dissolved NOM (including humic substances and microbially produced extracellular polymeric materials) [44,46,50]; and the concentration and type of electron donor [51–53]. Many of these parameters are interdependent (e.g., the rate of Fe(III) reduction may be controlled by the metabolic constraints placed on a given DIRB by the type and amount of electron donor available or by the system pH), often making it difficult to determine their relative contributions to the formation of specific Fe(II)-bearing secondary minerals.

The taxonomic diversity of DIRB is reflected in the broad range of electron donors that support DIR [54]; however, the effects of specific electron donors on the distribution of biogenic Fe(II) phases produced during DIR have not been extensively studied. The bioreduction of akaganeite (β-FeOOH) by *Shewanella* sp. HN-41 resulted in the formation of magnetite, siderite, and a combination of magnetite and siderite when lactate, pyruvate, and formate, respectively, were provided as electron donors [52]. Salas et al. [53] reported formation of siderite, green rust, and a combination of green rust and magnetite during DIR of ferrihydrite by *Shewanella putrefaciens* W3-18-1 with pyruvate, uridine, and lactate, respectively, as electron donors. Both of these studies show a pronounced effect of specific electron donors on the formation of specific secondary minerals. However, in each case only three donors were investigated, thus additional studies examining a broader range of electron donors are needed to develop a more comprehensive understanding of the key factors that determine the distribution of Fe(II)-bearing secondary minerals resulting from DIR of Fe(III) oxides.

In this study we examine the ability of *Shewanella putrefaciens* CN32 to utilize a broad range of potential electron donors for anaerobic respiration using Fe(III) oxide as an electron acceptor for anaerobic respiration. Formation of Fe(II)-bearing secondary minerals was determined using X-ray diffraction (XRD), ^{57}Fe Mössbauer spectroscopy, and scanning electron microscopy (SEM).

2. Materials and Methods

2.1. Experimental Setup

The organic electron donor survey experiment was conducted in sterile 160-mL serum bottles containing 100 mL of sterile defined mineral medium (DMM) [55] with Fe(III) as lepidocrocite (80 mM; Bayferrox 943, LANXESS Corp., Leverkusen, Germany/Pittsburgh, PA, USA), electron donor (75 mM acetate, L-alanine, citrate, ethanol, formate, D-glucose, L-glutamate, glycerol, glycine, DL-lactate, malate, N-acetyl glucosamine (NAG), propionate, pyruvate, L-serine, or succinate), and 100 μM 9,10-anthraquinone 2,6 disulfonate (AQDS). Characterization of the lepidocrocite used in this study is

provided in O'Loughlin et al. [28] The DMM was prepared by combining all components (except the electron donor and AQDS), the pH was adjusted to 7.5 by titration with 1 M NaOH, portioned into serum bottles, and autoclaved. After the medium cooled to ambient temperature, the electron donor and AQDS were added from filter-sterilized stock solutions. The bottles were sealed with rubber septa and aluminum crimp caps and made anoxic by sparging with sterile argon. Additional experiments with select organic electron donors (i.e., donors that supported DIR in the survey experiment) were conducted in 250-mL serum bottles containing 200 mL of DDM prepared in the same manner as described above and amended with either 25 mM NaCl or 25 mM Na_2SO_4. Bottles in which H_2 was provided as the electron donor were prepared in a similar manner but with 50 mL of DMM (amended with 25 mM of either NaCl, $NaHCO_3$, or Na_2SO_4) in 500-mL serum bottles and the headspace was flushed with sterile H_2 after sparging with argon (resulting in >20 mmol H_2). An additional set of bottles with H_2 as the electron donor was prepared containing 0.5 g of sterile Pd catalyst (0.5 wt % Pd on 3.2-mm alumina pellets) and 25 mM $NaHCO_3$. All experimental systems were prepared in triplicate.

The inoculum was prepared from late-log-phase cultures of *S. putrefaciens* CN32 (American Type Culture Collection BAA-543) as described by O'Loughlin et al. [16]. Experiments were initiated by spiking each bottle with the volume of inoculum needed to achieve a cell density of 5×10^9 cells mL^{-1}. The bottles were placed on a roller drum and incubated at 30 °C in the dark. Samples of the suspensions—for monitoring pH, Fe(II) production, and consumption of electron donors as well as for identification of secondary minerals by X-ray diffraction (XRD), scanning electron microscopy (SEM), and ^{57}Fe Mössbauer spectroscopy—were collected with sterile syringes. Unless otherwise indicated, sample collection and processing were conducted in a glove box containing an anoxic atmosphere (95% N_2 with 5% H_2).

2.2. Analytical Methods

The reduction of Fe(III) was monitored by measuring the total Fe(II) content of 0.75 M HCl extracts of the suspensions ($Fe(II)_{tot}$, referred to hereafter as Fe(II)). Samples for Fe(II) analysis were prepared by adding 0.75 mL of anoxic 1 M HCl to 0.25 mL of suspension. After 1 week, the samples were centrifuged at 25,000× *g* for 10 min. The Fe(II) concentrations in the supernatants were determined by the ferrozine assay [56]. Briefly, 1 mL of HEPES-buffered ferrozine reagent [57] was added to 50 µL of supernatant, and the absorbance at 562 nm was measured.

The disappearance of lepidocrocite and the formation of secondary minerals were monitored by powder X-ray diffraction (pXRD) with a Rigaku MiniFlex X-ray diffractometer (Rigaku Corporation, Tokyo, Japan) with Ni-filtered Cu Kα radiation. Samples for pXRD analysis were collected by filtration on 25-mm, 0.22-µm nylon filters and covered with 8.4-mm-thick Kapton® film under anoxic conditions; although the pXRD analysis was conducted under ambient atmosphere, samples prepared in this manner showed no evidence of oxidation when scanned between 5° and 80° 2θ at a speed of 1.25° 2θ min^{-1}. The pXRD patterns were analyzed with the JADE 7 software package (MDI, Livermore, CA, USA) to remove the background through polynomial fitting and also to remove the $K\alpha_2$ components. Samples of the filtrate were saved for pH measurement, measurement of dissolved Fe(II) [$Fe(II)_{aq}$)] using the ferrozine assay, and for analysis of organic electron donors using an Agilent 1100 series HPLC equipped with a UV-Vis absorbance detector (Agilent Technologies, Inc., Santa Clara, CA, USA). The samples for HPLC analysis were diluted with an equal volume of 10 mM H_2SO_4, and 50 µL of the diluted sample was injected on a Bio-Rad Aminex HPX-87H ion-exchange column (7.8 × 300 mm, Bio-Rad Laboratories Inc., Hercules, CA, USA). The column was eluted isocratically with 5 mM H_2SO_4 at a flow rate of 0.6 mL min^{-1} at 50 °C with analyte detection at 210 nm. The pH was measured with a precision of 0.01 using a Semi Micro pH electrode (Thermo Fisher Scientific Inc., Waltham, MA, USA) calibrated with NIST-traceable pH standards.

Samples for SEM imaging were prepared by placing 500 µL of suspension on aluminum specimen mounts, allowing the solids to settle, removing the overlying liquid with a pipette, and drying the film

of solids in a glove box. Specimens were briefly (<30 s) exposed to air during transfer to the Hitachi S-4700-II FEG-SEM (Hitachi High-Technologies Corporation, Tokyo, Japan).

Transmission Mössbauer spectroscopy was performed with a variable temperature He-cooled system with a 1024 channel detector. The ^{57}Co source used (~50 mCi) was in a Rh matrix at room temperature. All center shifts reported are relative to an α-Fe foil at room temperature. Samples were prepared by filtering the suspension (approximately 4 mL) in an anoxic glove box with recoverable filter paper. The filter paper was then sealed between two pieces of 5 mm Kapton tape to avoid oxidation while the sample was mounted. No indication of inadvertent oxidation was observed. Spectral fitting was done using Recoil Software version 1.01998 (University of Ottawa, Ottawa, ON, Canada). Voigt-based fitting was used to model the spectra to determine the hyperfine parameters and the relative areas between phases. The Lorentzian linewidth was held at 0.12 mm s^{-1}, as it was the linewidth measured on the spectrometer for an ideally thick α-Fe foil. The relative peak areas (1:1 for doublets, 3:2:1:1:2:3 for sextets) were held constant throughout fitting. Each phase was fitted with only a single component (i.e., multiple QS and H distributions were not allowed for a single phase in fitting).

2.3. Thermodynamic Modeling

Geochemical models of the Fe-C system were created using The Geochemist's Workbench software suite (version 8.0.12, Aqueous Solutions LLC, Champaign, IL, USA) [58]. The program Act2 was used to create Pourbaix (Eh-pH) diagrams showing the stability fields of the minerals that would be expected to form across a range of likely conditions for these microcosms. Thermodynamic data was obtained from the "thermo.dat" database in The Geochemist's Workbench [59] with the addition of lepidocrocite [60], carbonate green rust [61], and ferrous hydroxycarbonate [62].

Eh-pH diagrams were constrained by the activity of ferrous iron (a[Fe^{2+}]) and bicarbonate (a[HCO_3^-]) as calculated using the program React with the components of DMM as basis species. Ferrous and ferric minerals not observed to form in the system (hematite, magnetite, goethite, wüstite) were suppressed. The value of a[HCO_3^-] was modeled by adding it as a simple reactant at pH 7.5, the initial starting pH of the system. As the concentration of HCO_3^- was not measured directly during the experiments, a range of possible a[HCO_3^-] was calculated and used to create separate Eh-pH diagrams to examine the effect of the range of a[HCO_3^-] on the stability of secondary iron minerals.

3. Results

3.1. Electron Donor Survey

The production of Fe(II) by *S. putrefaciens* CN32 in the presence of lepidocrocite and a broad range of potential electron donors is shown in Figure 1. In the absence of an exogenous electron donor, lepidocrocite reduction by *S. putrefaciens* CN32 was limited; within 72 days only 3.6 mM Fe(II) was produced. Systems amended with acetate, alanine, citrate, ethanol, glucose, glutamate, glycerol, glycine, malate, propionate, or succinate showed slightly higher levels of Fe(II) production (<7 mM). Significantly greater Fe(II) production was observed in systems amended with formate (58 mM), lactate (57 mM), H_2, (18 mM), NAG (61 mM), pyruvate (57 mM), and serine (58 mM); DIR by *S. putrefaciens* CN32 using these electron donors was examined in greater detail in a more focused set of experiments, the results of which follow.

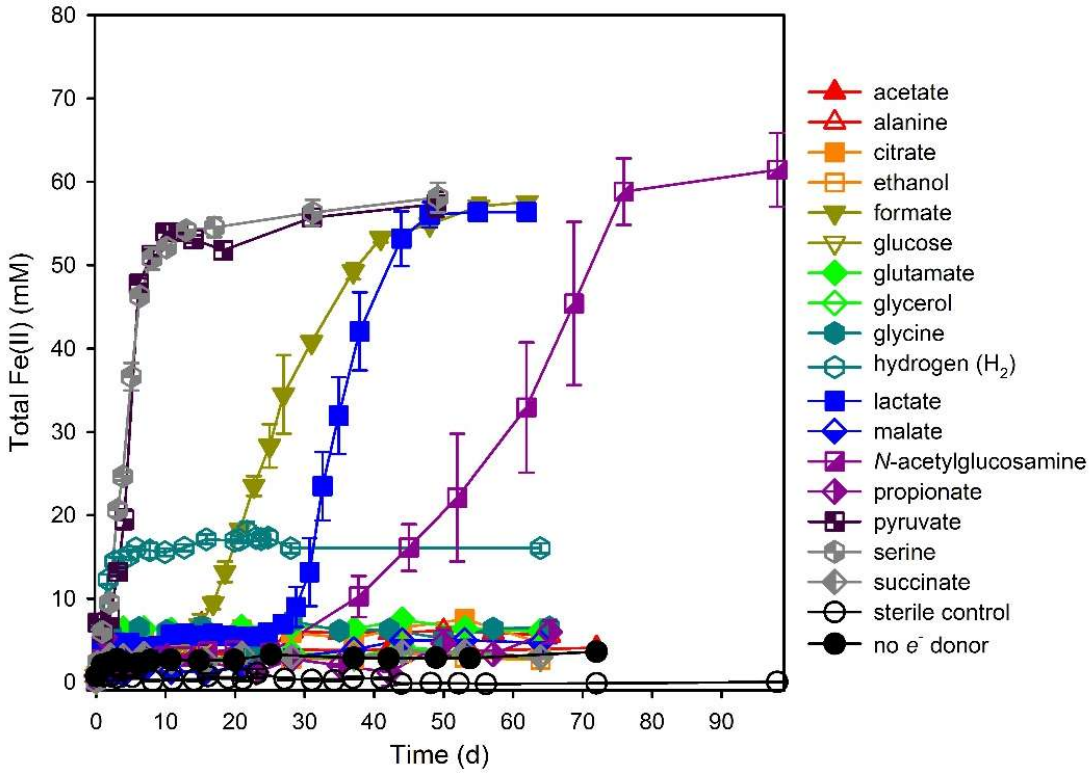

Figure 1. Fe(II) production during the bioreduction of lepidocrocite by *S. putrefaciens* CN32 as a function of available electron donor.

3.2. Hydrogen

Fe(II) production by *S. putrefaciens* CN32 was essentially immediate with H_2 as the electron donor (Figure 2). The presence of specific anions had a significant effect on both the rate and extent of Fe(II) production, which were highest in the presence of carbonate (Table 1). Fe(II) concentrations approached steady state within 3 days and were largely unaffected by replenishment of headspace H_2 or re-inoculation with freshly cultured *S. putrefaciens* CN32. Moreover, substantially higher levels of Fe(II) were observed in the abiotic system containing Pd catalyst as an abiotic surrogate for microbial reduction of lepidocrocite (either by direct reduction or indirect reduction involving AQDS as an electron shuttle). In all systems the pH increased commensurate with the extent of Fe(II) production. Green rust was the only secondary mineral identified by pXRD and Mössbauer spectroscopy (Tables 2 and 3, Figure 3). Carbonate green rust formed in the chloride- and carbonate-amended systems and sulfate green rust formed in the sulfate-amended system (Figure 3). The solids consisted primarily of platy hexagonal particles up to 5 µm across, covered in tabular submicron-sized particles of unreacted lepidocrocite (Figure 4A,B).

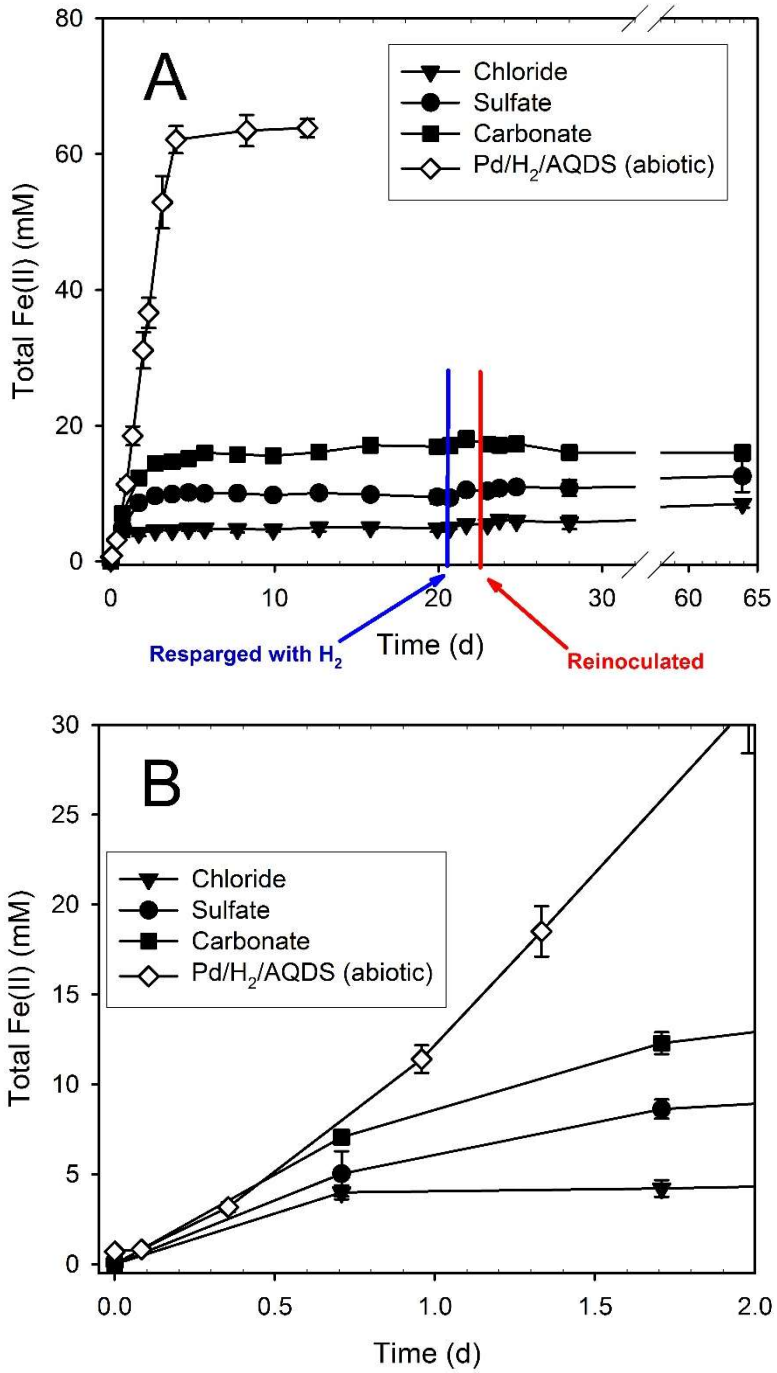

Figure 2. (**A**) Fe(II) production during the bioreduction of lepidocrocite by *S. putrefaciens* CN32 using H_2 as an electron donor in the presence of either chloride, sulfate, or carbonate, compared to abiotic reduction of lepidocrocite by H_2 in the presence of Pd catalyst, the electron shuttle 9,10-anthraquinone 2,6 disulfonate (AQDS), and carbonate and (**B**) an expanded view of Fe(II) production within the first 2 days. Error bars indicate one standard deviation.

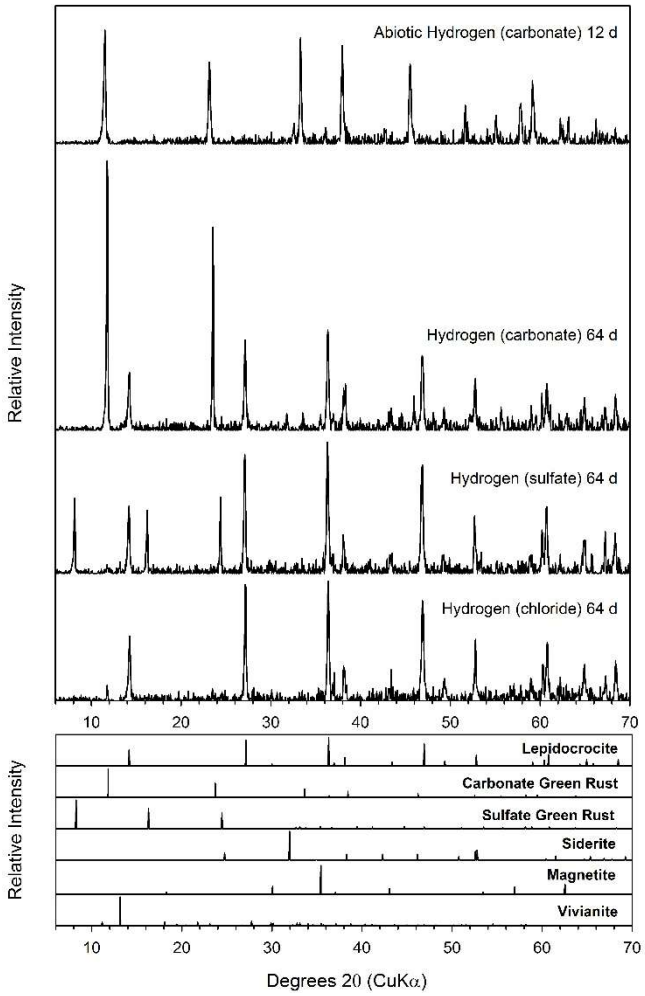

Figure 3. Powder X-ray diffraction analysis of the solids in the H_2-amended systems at the end of the incubations.

Table 1. Final pH, Fe(II), and acetate concentrations, maximum Fe(II) production rates, and e^- donor consumption ratios.

System	Final [a] pH	Final $Fe(II)_{aq}$ (mM)	Final $Fe(II)_{tot}$ (mM)	$Fe(II)_{tot}$ Production during Bioreduction [c] (mmol d^{-1})	e^- Donor Consumed (mM)	$Fe(II)_{tot}$:e^- Donor Consumed
Formate (chloride)	9.05 ± 0.01	0.8 ± 0.1	57.6 ± 0.2	2.32 ± 0.09	27.7 ± 1.4	2.1
Formate (sulfate)	9.06± 0.05	0.7 ± 0.1	55.1 ± 2.4	1.39 ± 0.09	25.3 ± 1.9	2.2
H_2 abiotic	9.30 ± 0.01	ND [b]	63.8 ± 1.3	16.36 ± 0.52	ND	ND
H_2 (carbonate)	8.83 ± 0.13	0.8 ± 0.1	16.0 ± 0.6	7.07 ± 1.31	ND	ND
H_2 (sulfate)	8.59 ± 0.09	0.9 ± 0.1	12.6 ± 2.3	7.09 ± 0.97	ND	ND
H_2 (chloride)	8.36 ± 0.11	1.2 ± 0.3	8.5 ± 0.6	5.64 ± 0.95	ND	ND
Lactate (chloride)	8.01 ± 0.01	4.7 ± 0.1	56.4 ± 0.8	3.76 ± 0.23	22.6 ± 1.3	2.5
Lactate (sulfate)	8.23 ± 0.03	2.9 ± 0.1	59.3 ± 4.8	3.18 ± 0.12	22.6 ± 1.4	2.6
NAG (chloride)	7.55 ± 0.10	6.8 ± 2.2	61.4 ± 4.4	1.31 ± 0.14	38.4 ± 2.8	1.6
NAG (sulfate)	7.69 ± 0.04	6.8 ± 0.7	70.6 ± 3.7	1.57 ± 0.24	40.9 ± 2.1	1.7
Pyruvate (chloride)	8.47 ± 0.05	2.0 ± 0.1	57.3 ± 1.5	9.84 ± 1.63	75	0.8
Pyruvate (sulfate)	8.44 ± 0.04	1.8 ± 0.2	59.3 ± 5.7	10.20 ± 1.91	75	0.8
Serine (chloride)	8.17 ± 0.02	2.3 ± 0.1	58.1 ± 1.8	7.25 ± 0.34	75	0.8
Serine (sulfate)	8.46 ± 0.29	1.4 ± 1.0	61.0 ± 7.0	8.38 ± 0.28	75	0.8

[a] Final measurements were made at 49 days after inoculation in the pyruvate and serine systems, at 62 days in the formate and lactate systems, 64 days in the hydrogen systems, and at 106 days in the NAG systems; [b] Not determined (ND); [c] Fe(II) production rates were calculated by linear regression using least-squares regression of the data during the period of maximum sustained Fe(II) production.

Table 2. Fit parameters from Mössbauer analysis of the secondary minerals.

Sample	Temp (K)	CS (mm s^{-1})	QS (mm s^{-1})	H (T)	Mineral	RA (%)
Formate (chloride)	77	1.26	2.83	-	Green Rust Fe(II)	70.5
	-	0.48	0.38	-	Green Rust Fe(III)	29.5
	13	1.27	2.80	-	Green Rust Fe(II)	69.9
	-	0.49	0.37	-	Green Rust Fe(III)	30.1
Formate (sulfate)	77	1.26	2.85	-	Green Rust Fe(II)	68.1
	-	0.47	0.40	-	Green Rust Fe(III)	31.9
	13	1.26	2.82	-	Green Rust Fe(II)	67.6
	13	0.47	0.41	-	Green Rust Fe(III)	32.4
Lactate (chloride)	77	1.27	2.85	-	Green Rust Fe(II)	66.7
	-	0.47	0.41	-	Green Rust Fe(III)	33.3
	13	1.27	2.82	-	Green Rust Fe(II)	69.4
	-	0.48	0.38	-	Green Rust Fe(III)	30.6
Lactate (sulfate)	77	1.26	2.89	-	Green Rust Fe(II)	61.9
	-	0.45	0.46	-	Green Rust Fe(III)	38.1
	13	1.26	2.88	-	Green Rust Fe(II)	58.8
	-	0.41	0.51	-	Green Rust Fe(III)	41.2
NAG (chloride)	77	1.36	2.05	-	Siderite	17.7
	-	1.27	2.88	-	Green Rust Fe(II)	47.4
	-	0.48	0.42	-	Green Rust Fe(III)	13.2
	-	0.49	0.6	-	Lepidocrocite	21.4
	13	1.33	2.09	16.8	Siderite	14.7
	-	1.28	2.84	-	Green Rust Fe(II)	46.4
	-	0.5	0.4	-	Green Rust Fe(III)	18.3
	-	0.49	0.03	45.3	Lepidocrocite	20.6
NAG (sulfate)	77	1.35	2.04	-	Siderite	20.9
	-	1.27	2.91	-	Green Rust Fe(II)	50
	-	0.42	0.55	-	Green Rust Fe(III)	29.1
	13	1.35	2.1	16.8	Siderite	29.4
	-	1.28	2.91	-	Green Rust Fe(II)	41.5
	-	0.43	0.56	-	Green Rust Fe(III)	29.1
Pyruvate (chloride)	77	1.36	2.11	-	Siderite	38.7
	-	1.33	2.76	-	Siderite 2	33.8
	-	0.48	0.56	-	Lepidocrocite	27.5
	13	-	-	-	-	-
		No quantitation can be made—siderite and lepidocrocite present				
Pyruvate (sulfate)	77	1.36	2.09	-	Siderite	38.7
	-	1.33	2.79	-	Siderite 2	30.6
	-	0.48	0.57	-	Lepidocrocite	30.7
	13	-	-	-	-	-
		No quantitation can be made—siderite and lepidocrocite present				
Serine (chloride)	77	1.36	2.08	-	Siderite	43
	-	1.33	2.77	-	Siderite 2	33.3
	-	0.48	0.56	-	Lepidocrocite	23.6
	13	-	-	-	-	-
		No quantitation can be made—siderite and lepidocrocite present				
Serine (sulfate)	77	1.36	2.08	-	Siderite	43
	-	1.33	2.77	-	Siderite 2	33.3
	-	0.48	0.56	-	Lepidocrocite	23.6
	13	-	-	-	-	-
		No quantitation can be made—siderite and lepidocrocite present				
H_2 (chloride)	77	1.23	2.87	-	Green Rust Fe(II)	19.9
	-	0.43	0.53	-	Green Rust Fe(III)	7.7
	-	0.5	0.6	-	Lepidocrocite	72.4
	13	-				
		No quantitation can be made—green rust and lepidocrocite present				
H_2 (carbonate)	77	1.25	2.78	-	Green Rust Fe(II)	32.2
	-	0.5	0.37	-	Green Rust Fe(III)	18.7
	-	0.49	0.62	-	Lepidocrocite	49.1
	13	1.27	2.85	-	Green Rust Fe(II)	8.5
	-	0.48	0.38	-	Green Rust Fe(III)	3.3
	-	0.50	0.01	45.3	Lepidocrocite	88.2
H_2 (sulfate)	77	1.28	2.88	-	Green Rust Fe(II)	16.1
	-	0.49	0.41	-	Green Rust Fe(III)	19.0
	-	0.49	0.59	-	Lepidocrocite	65.0
	13	-	-	-	-	-
		No quantitation can be made—predominantly lepidocrocite				

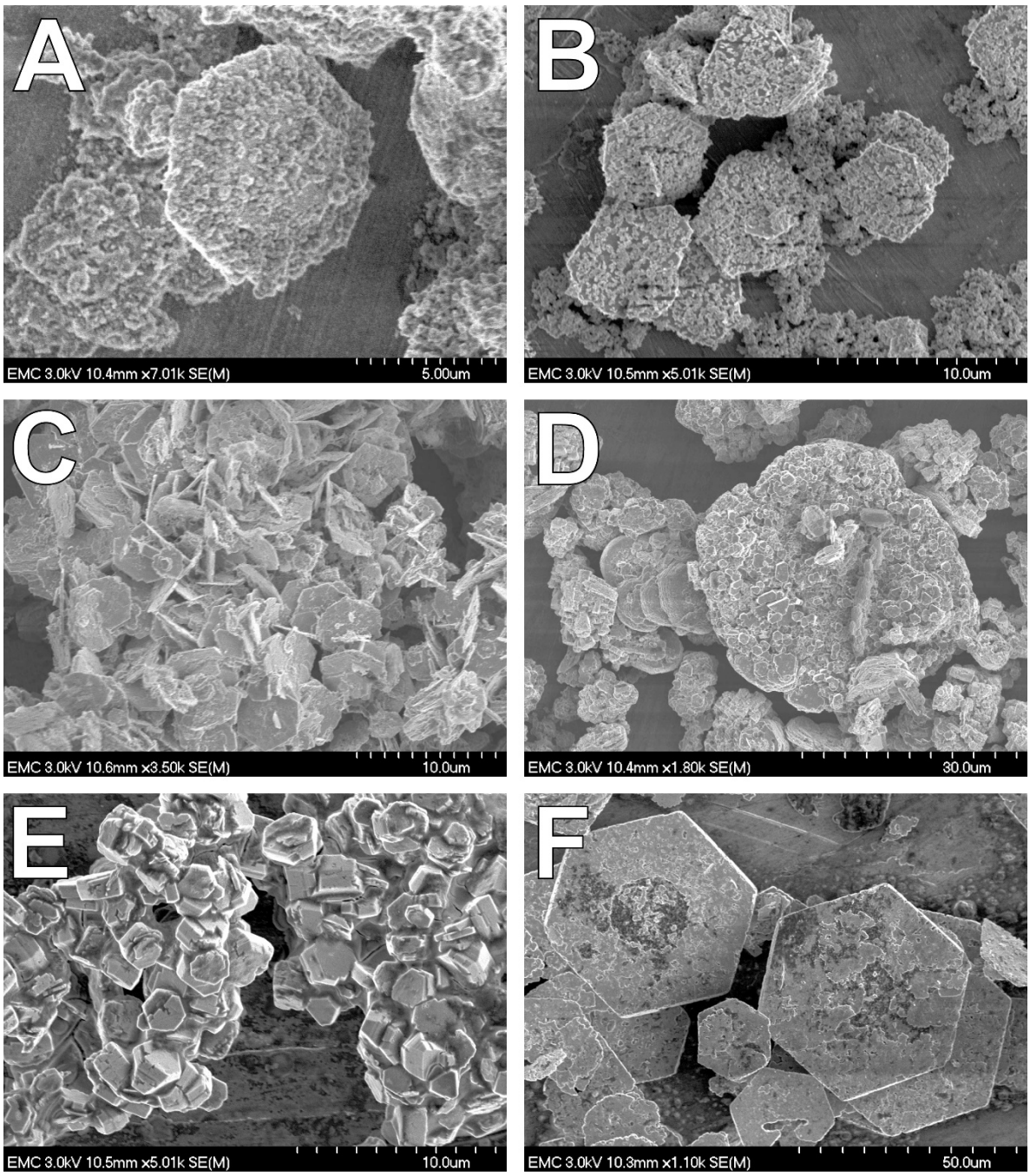

Figure 4. SEM images of solids at the end of the incubations containing H_2 with sulfate (**A**), H_2 with carbonate (**B**), formate with chloride (**C**), formate with sulfate (**D**), lactate with chloride (**E**), and lactate with sulfate (**F**).

Table 3. Identification of secondary minerals.

System	pXRD	Mössbauer	SEM
Formate (chloride)	GR_C [a]	GR	GR
Formate (sulfate)	GR_C	GR	GR
H_2 abiotic	GR_C	ND	ND
H_2 (carbonate)	GR_C	GR	GR
H_2 (sulfate)	GR_S [a]	GR	GR
H_2 (chloride)	GR_C	GR	GR
Lactate (chloride)	GR_C	GR	GR
Lactate (sulfate)	GR_C, GR_S	GR	GR
NAG (chloride)	GR_C, Sid [b]	GR, Sid	GR, Sid
NAG (sulfate)	GR_C, GR_S, Sid	GR, Sid	GR, Sid
Pyruvate (chloride)	Sid	Sid	Sid
Pyruvate (sulfate)	Sid	Sid	Sid
Serine (chloride)	Sid	Sid	Sid
Serine (sulfate)	Sid	Sid	Sid

[a] Carbonate green rust (GR_C) and sulfate green rust (GR_S); [b] Siderite (Sid).

3.3. Formate

Formate essentially served as a positive control given that we have previously shown that formate is utilized as an electron donor for DIR by *S. putrefaciens* CN32 [16,28,44,55,63]. The initial production of 2.3 mM Fe(II) within the first 24 h was followed by a lag period lasting ~13 days in the chloride-amended system, after which there was vigorous and sustained Fe(II) production concurrent with formate consumption (Figure 5). The reduction of Fe(III) was essentially complete (i.e., there was no change in Fe(II) concentrations) by day 55. The systems were not explicitly buffered (i.e., a buffer was not a component of the DMM) and the pH increased from 7.5 to 8.3 within 18 h after inoculation followed by a slower pH increase, ultimately reaching pH 9.1 by day 62 (Figure 5). The bioreduction of lepidocrocite in the sulfate-amended systems followed similar trends with respect to Fe(II) production, formate consumption and pH, but with a longer lag period (Figure 5) and slower rate of total Fe(II) production (Table 1). Analysis of the solids by pXRD (Figure 6) and Mössbauer spectroscopy (Table 2) indicates complete removal of lepidocrocite accompanied by the formation of green rust. Carbonate green rust was the only secondary mineral observed in the chloride-amended system (Figure 6), present as platy hexagonal particles up to 5 μm across, often with well-defined edges (Figure 4C). In the sulfate-amended systems, indications of sulfate green rust were observed by day 9, by day 15 both sulfate and carbonate green rust were present, and by day 62 only carbonate green rust was detected (Figure 6). Unlike the generally well-formed crystallites in the chloride-amended system, the green rust particles in the sulfate-amended system were highly irregular, both in terms of width as well as the morphology of the crystal edges (Figure 4D).

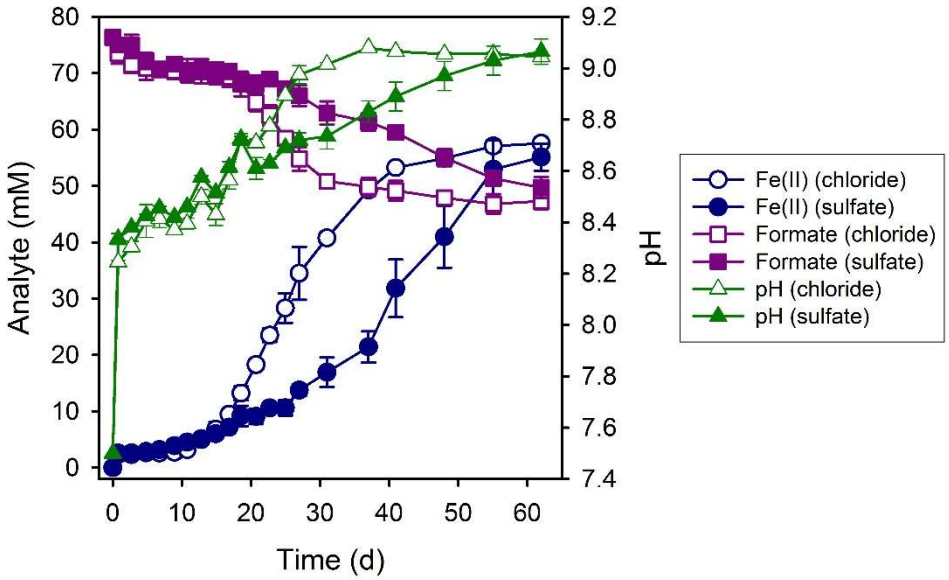

Figure 5. Fe(II) production, formate consumption, and pH during the bioreduction of lepidocrocite by *S. putrefaciens* CN32 with formate as the electron donor.

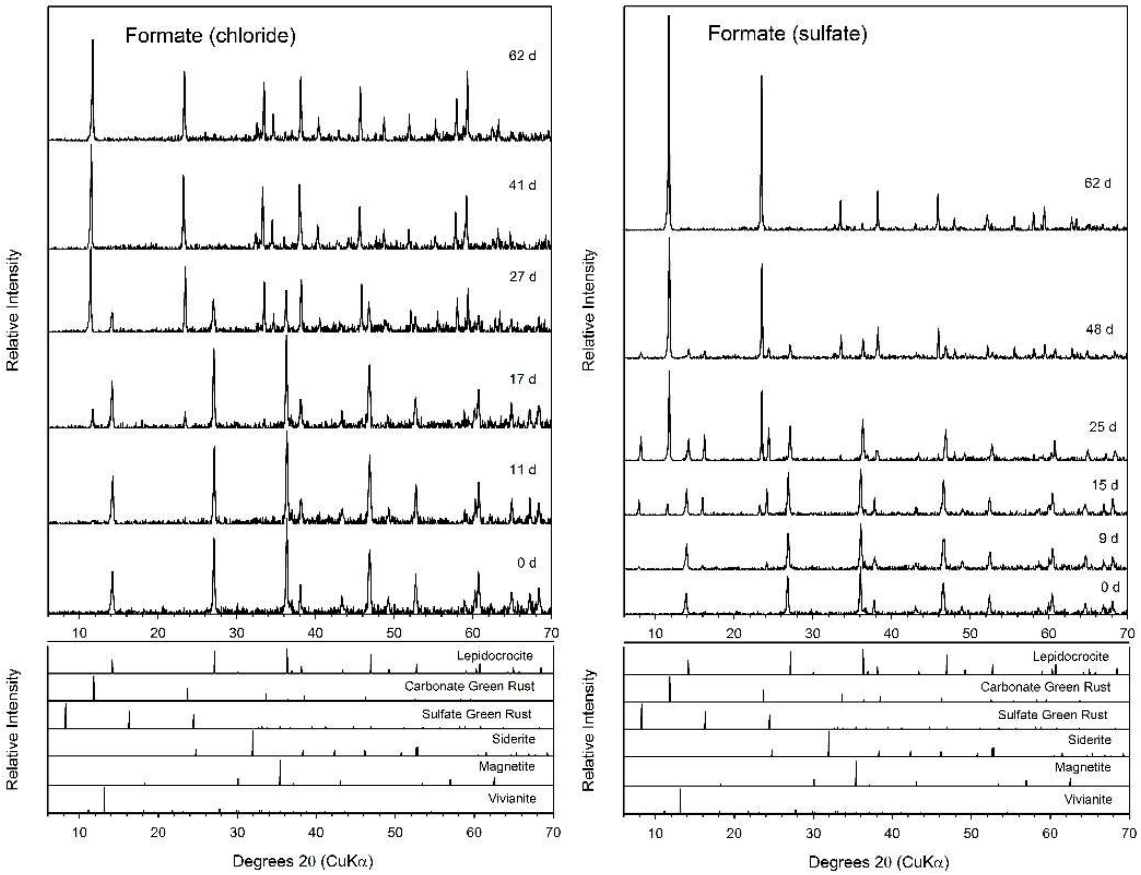

Figure 6. pXRD analysis of the solids in the systems with formate as the electron donor amended with chloride (**left**) or sulfate (**right**).

3.4. Lactate

As observed with formate, there was an initial increase in pH from 7.5 to 8.2 and a pulse of Fe(II) production (~4 mM) within the first 24 h, that was followed by a lag in Fe(II) production lasting ~27 days and ~17 days in the chloride- and sulfate-amended systems, respectively (Figure 7). After the corresponding lag periods, Fe(II) production proceeded at similar rates (Table 1) in each system leading to production of 56 and 59 mM total Fe(II) in the chloride- and sulfate-amended systems, respectively. Unlike the formate systems, there was no further increase in pH after the initial rise; indeed, by day 62 the pH decreased to 8.0 in the chloride-amended system (Figure 7). Lactate consumption was concurrent with Fe(II) and acetate production. At the end of the experiment (day 62) both pXRD and Mössbauer spectroscopy showed complete loss of lepidocrocite and formation of green rust (Table 2 and Figure 8). Carbonate green rust was the only secondary mineral observed in the chloride-amended system (Figure 8) and the crystallites were 1–2 μm thick and up to 2 μm wide and nominally hexagonal (Figure 4E). In the sulfate-amended systems, indications of sulfate green rust were observed by day 7, and by day 17 both sulfate and carbonate green rust were present (Figure 8); unlike the sulfate-amended formate system, both sulfate and carbonate green rust were present at the end of the experiment (day 62). The green rust crystallites in the sulfate-amended system were exceptionally wide (up to 50 μm), thin hexagonal plates with very well-formed edges (Figure 4F).

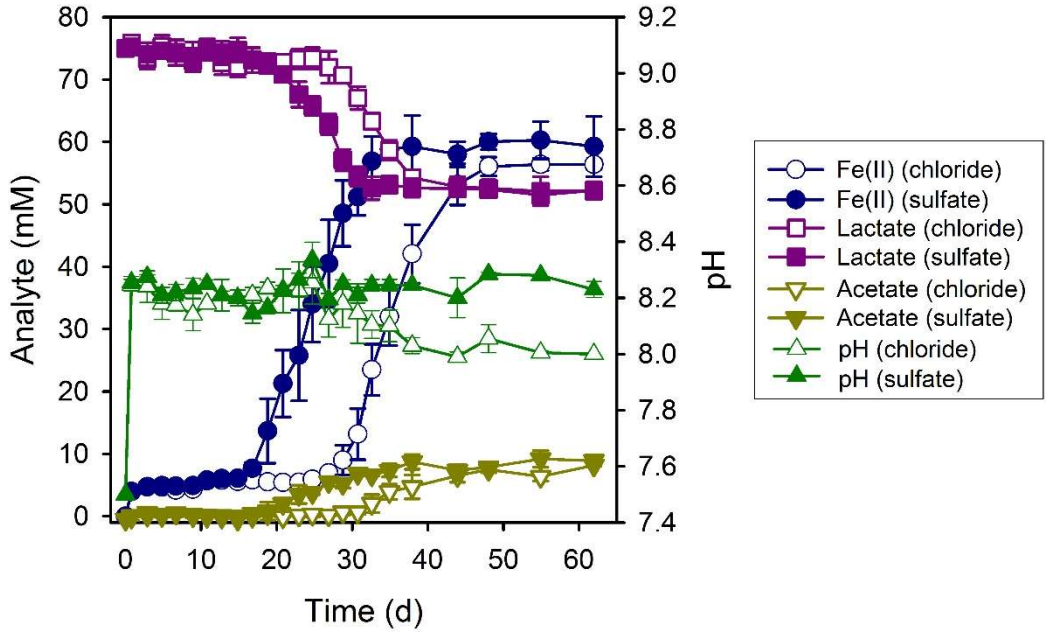

Figure 7. Fe(II) and acetate production, lactate consumption, and pH during the bioreduction of lepidocrocite by *S. putrefaciens* CN32 with lactate as the electron donor.

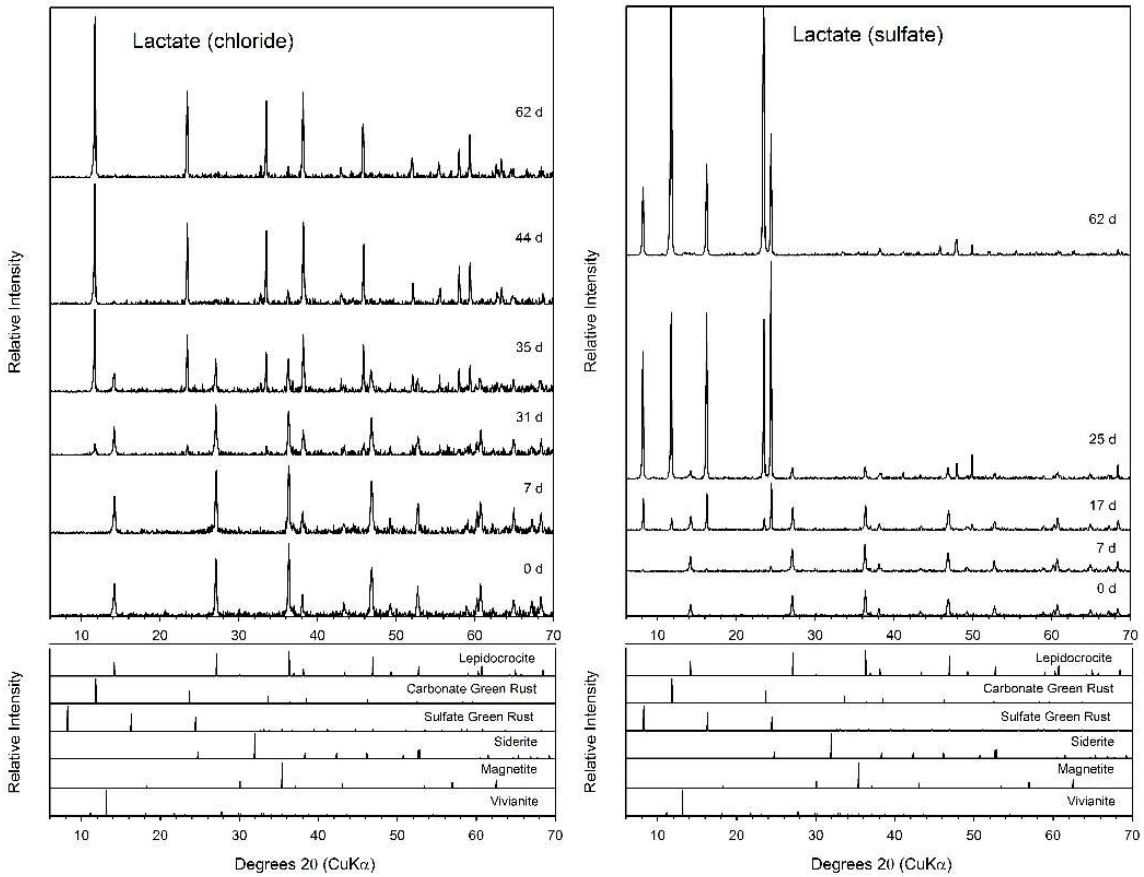

Figure 8. pXRD analysis of the solids in the systems with lactate as the electron donor amended with chloride (**left**) or sulfate (**right**).

3.5. N-Acetylglucosamine (NAG)

Within the first 24 h after inoculation, ~3 mM Fe(II) was produced in the chloride-amended system and there was minimal change over the next 24 days (Figure 9). Substantial Fe(II) production was observed between day 25 and day 76 leading to an accumulation of ~61 mM Fe(II) at the termination of the experiment at day 106; at which time pXRD and Mössbauer spectroscopy indicated the presence of residual lepidocrocite and secondary minerals siderite and carbonate green rust (Table 2 and Figure 10). Carbonate green rust formation was not evident until 38 days after inoculation and siderite was not observed until day 69 (Figure 10). The Fe(II) production profile was more complex in the sulfate-amended system (Figure 9). As with the chloride system, there was an initial production of Fe(II) within the first 24 h (~4 mM), but this was followed by a much shorter lag period (3 days), after which the Fe(II) concentration increased to 14 mM at day 25 and remained essentially unchanged until Fe(II) production resumed at day 31. At 106 days after inoculation, the Fe(II) concentration reached 71 mM, at which point lepidocrocite was no longer detected by Mössbauer or pXRD (Table 2 and Figure 10). Sulfate green rust formation was first observed at 7 days after inoculation, followed by the appearance of carbonate green rust at day 38 and siderite at day 69 (Figure 10). In both systems, Fe(II) production was accompanied by consumption of NAG and accumulation of acetate and after an initial increase in pH to ~8.1, the pH gradually decreased to ~7.6 by day 106 (Figure 9). The morphology of green rust crystallites were similar in both chloride- and sulfate-amended systems; thin hexagonal particles with irregular edges up to 20 μm wide decorated with anhedral to subhedral 0.5–2 μm rhombic siderite crystallites (Figure 11A,B).

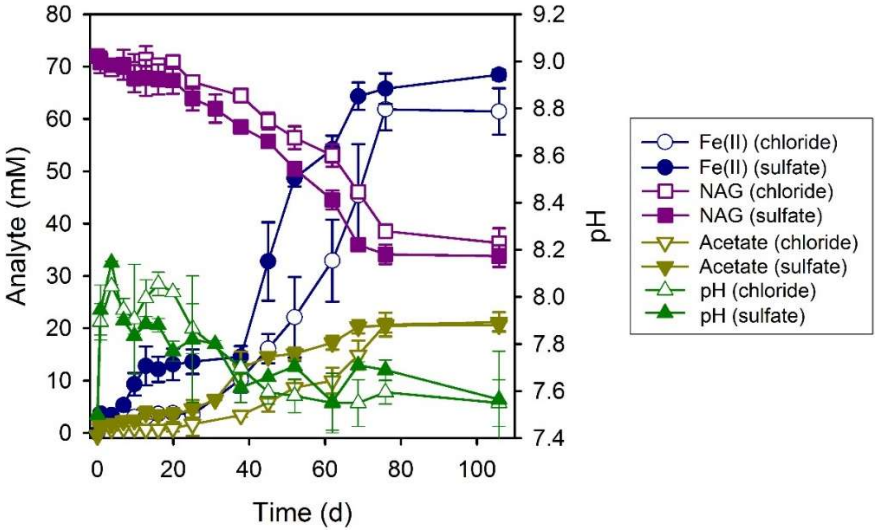

Figure 9. Fe(II) and acetate production, *N*-acetylglucosamine (NAG) consumption, and pH during the bioreduction of lepidocrocite by *S. putrefaciens* CN32 with NAG as the electron donor.

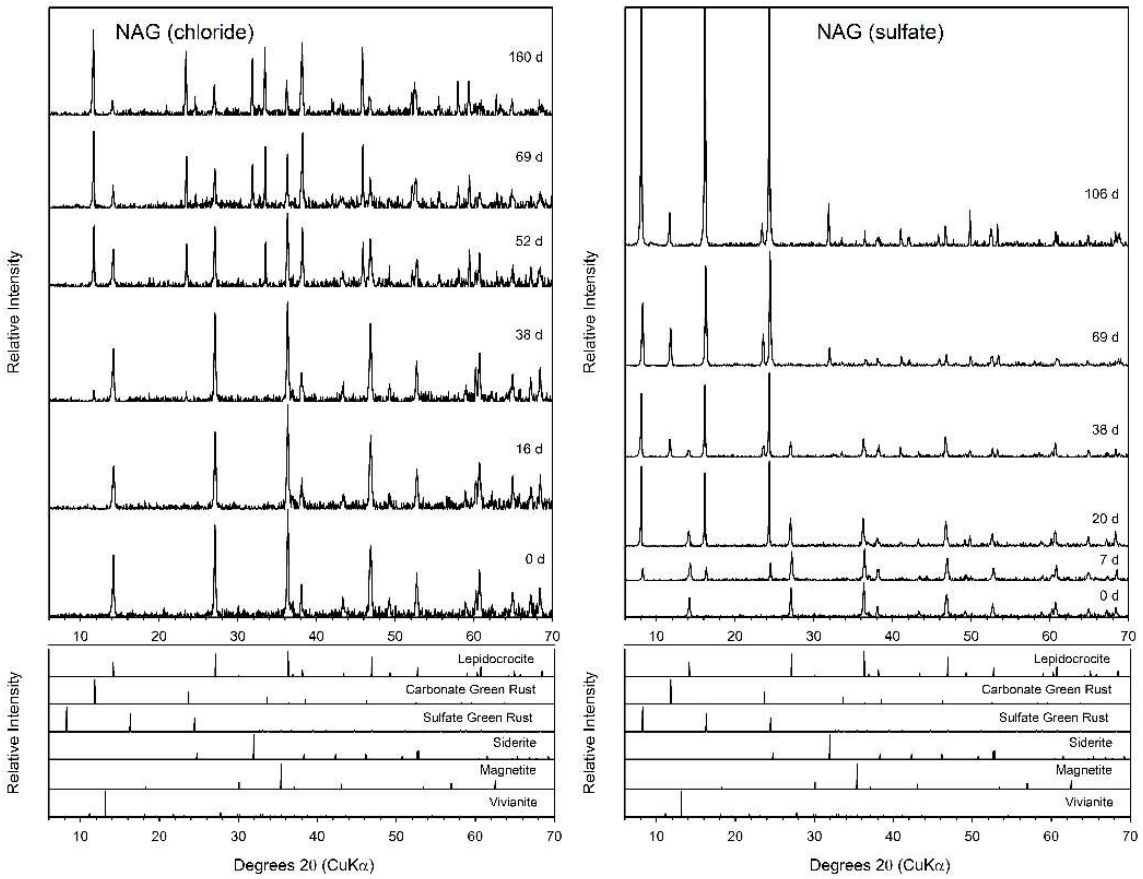

Figure 10. pXRD analysis of the solids in the systems with *N*-acetylglucosamine (NAG) as the electron donor amended with chloride (**left**) or sulfate (**right**).

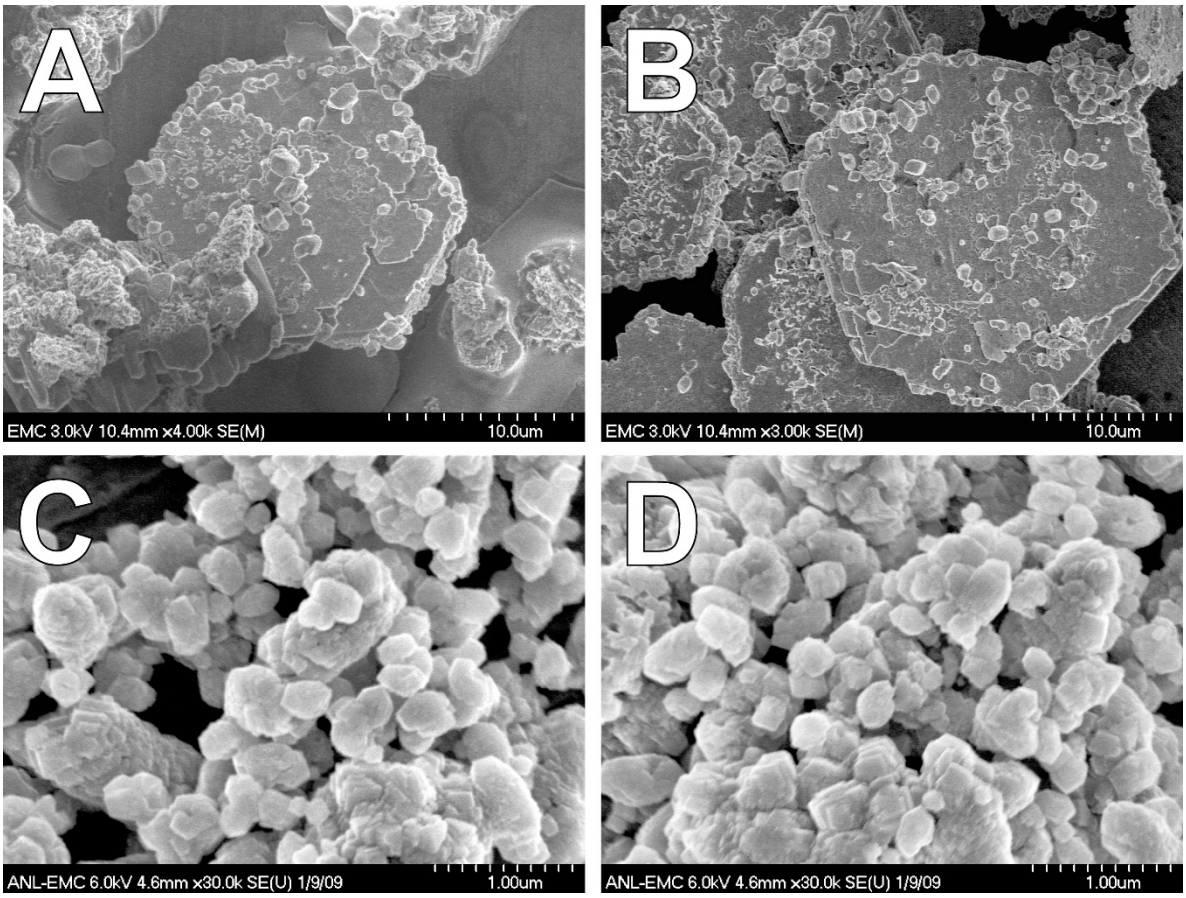

Figure 11. SEM images of solids at the end of the incubations containing *N*-acetylglucosamine (NAG) with chloride (**A**), NAG with sulfate (**B**), pyruvate with sulfate (**C**), and serine with sulfate (**D**).

3.6. Pyruvate

Compared to formate, lactate, and NAG, the initial Fe(II) production was higher with pyruvate (7 mM within 6.5 h) and the overall bioreduction of lepidocrocite was substantially faster, with >90% of the total Fe(II) production occurring within the first 10 days; both the chloride- and sulfate-amended systems followed essentially the same trajectory (Figure 12). Fe(II) production was accompanied by complete depletion of pyruvate and accumulation of acetate. The pH varied considerably over the course of the experiment. Within 6 h of inoculation, the pH increased from 7.5 to 8.0, followed by a decrease to 7.1 over the next 66 h, a rebound to pH 8 by day 6, and a gradual increase to a final pH of 8.5 by day 106 (Figure 12). The solids remaining at the end of the experiment consisted of residual lepidocrocite and siderite (Table 2 and Figure 13); there were no indications of green rust formation at any point during the experiment (data not shown). Siderite was present as anhedral to subhedral imperfect rhombohedral crystallites, typically 1–3 μm and often highly aggregated/cemented (Figure 11C).

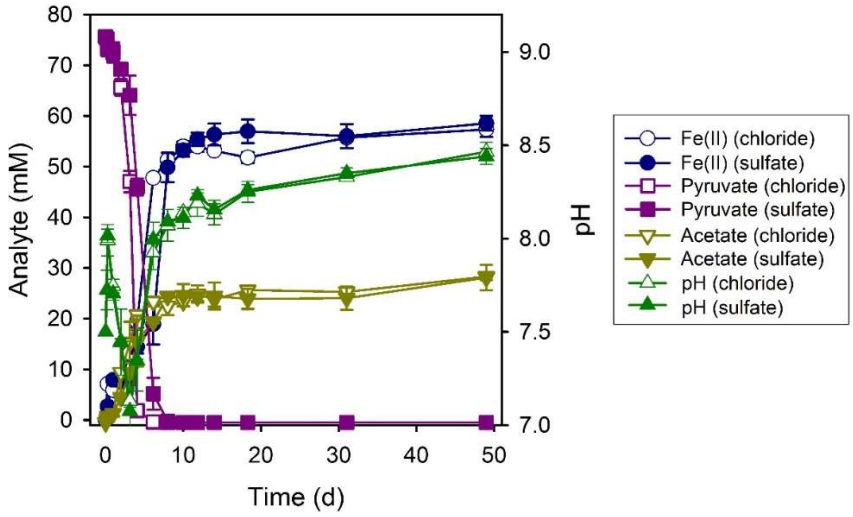

Figure 12. Fe(II) and acetate production, pyruvate consumption, and pH during the bioreduction of lepidocrocite by *S. putrefaciens* CN32 with pyruvate as the electron donor.

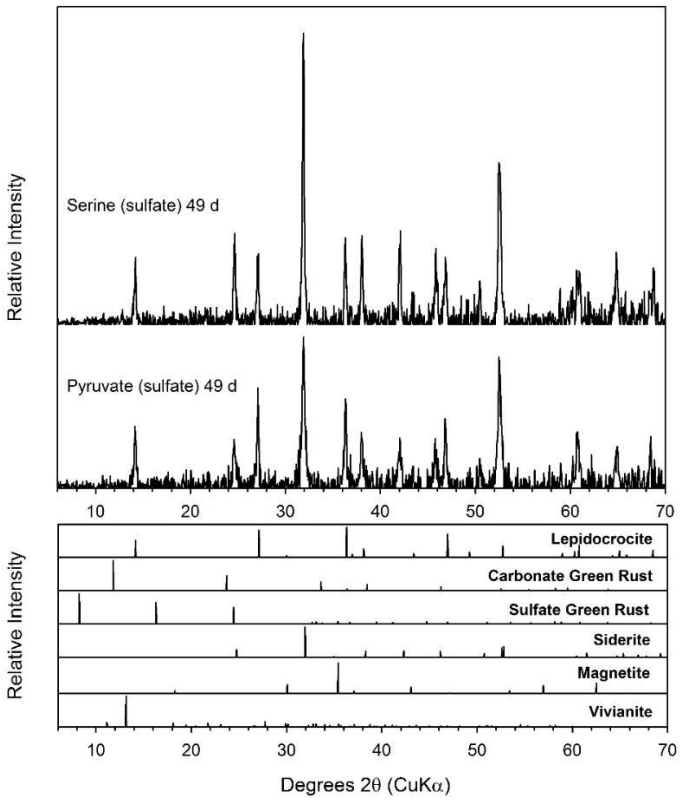

Figure 13. pXRD analysis of the solids in the sulfate-amended systems with pyruvate or serine as the electron donor.

3.7. Serine

The bioreduction of lepidocrocite by *S. putrefaciens* CN32 was immediate and sustained when serine was provided as the electron donor; nearly 90% of Fe(II) production occurred within the first 10 days in both the chloride- and sulfate-amended systems (Figure 14). We were unable to measure serine concentrations, but Fe(II) production was concurrent with acetate production, and pyruvate was observed as a transient species. As with pyruvate, the pH in the serine systems was variable over the course of the experiment, with final pH values of 8.2 and 8.5 in the chloride- and sulfate-amended systems, respectively. In both systems the solids at the conclusion of the experiment consisted of

residual lepidocrocite and siderite (Table 2 and Figure 13). The morphology of siderite particles formed in the serine systems were identical to those in the pyruvate systems (Figure 11C,D).

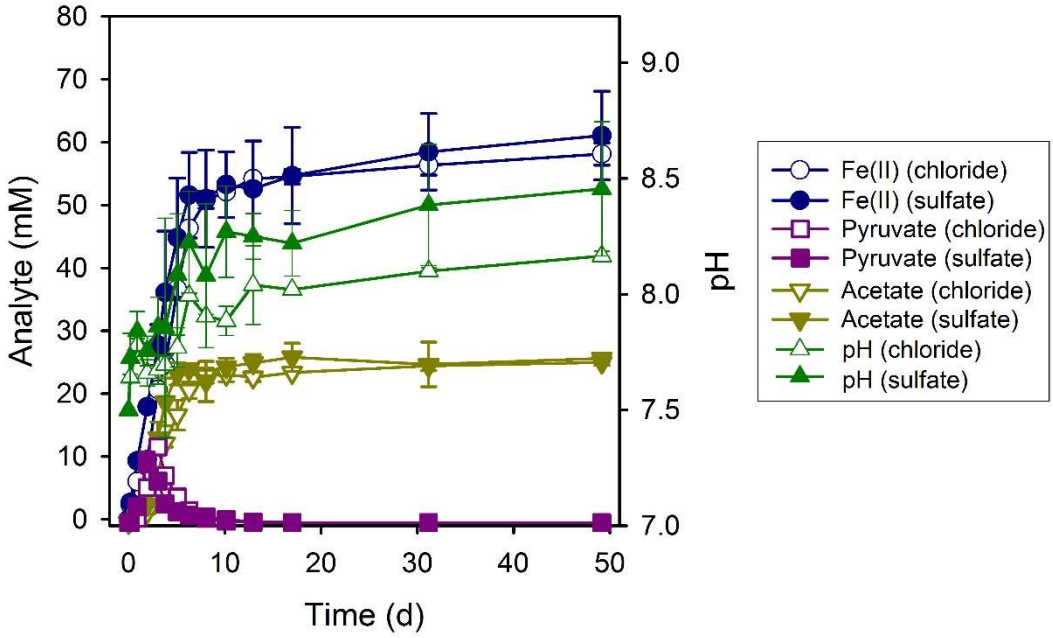

Figure 14. Fe(II), acetate, and pyruvate production/consumption and pH during the bioreduction of lepidocrocite by *S. putrefaciens* CN32 with serine as the electron donor.

4. Discussion

4.1. Electron Donor Utilization and Dissimilatory Iron(III) Reduction

The genus *Shewanella* consists of a phenotypically diverse group of over 50 species found widely distributed in a broad range of aquatic (lacustrine and marine) and terrestrial environments [64–66]. Under oxic conditions, members of the genus can utilize a broad range of $C_{1–3}$ aliphatic acids, amino acids, sugars, peptides, and nucleotides [65,67–69], but only a limited subset are utilized as electron donors for anaerobic respiration [70]. Among the 17 putative electron donors we tested with *S. putrefaciens* CN32, only H_2, formate, lactate, pyruvate, serine, and NAG supported anaerobic respiration with AQDS/Fe(III) oxide as the terminal electron acceptor(s).

The ability to use H_2 as an electron donor for DIR is broadly represented within *Shewanella* [71–76]. In this study, reduction of Fe(III) by *S. putrefaciens* CN32 was rapid within the first 2 days, then quickly plateaued to approximately 5, 10, and 15 mM Fe(II) in the chloride, sulfate, and carbonate systems, respectively. The limited extent of Fe(III) reduction is not due to electron donor limitation as the systems initially contained >20 mmol H_2 and only 4 mmol Fe(III) (50 mL of 80 mM Fe(III)). It is possible that hydrogen may have escaped from the bottle, thus limiting Fe(III) reduction; however, replenishing the hydrogen headspace did not result in significant additional Fe(II) production. Likewise, the limited Fe(II) production cannot be explained by a decrease in cell viability over time as reinoculation with freshly grown *S. putrefaciens* CN32 resulted in no increase in Fe(II). Furthermore, the production of ~60 mM Fe(II) within 4 days in the abiotic control (i.e., H_2/Pd/AQDS as a surrogate for microbial reduction) suggests that there was no thermodynamic limitation on the system. Limited reduction of Fe(III) was also observed during DIR of γ-FeOOH by *S. putrefaciens* CIP 8040^T with H_2 as the electron donor [76].

Formate and lactate are established electron donors for DIR by *S. putrefaciens* CN32 [25,33,44,48] as well as *Shewanella* spp. in general [16,34,46,52,53,71–75,77]. Consumption of formate by *S. putrefaciens* CN32 was directly linked to Fe(II) production. Approximately 2 moles of Fe(II) produced for each mole of formate consumed (Table 1) by *S. putrefaciens* CN32, consistent with the stoichiometry of formate

oxidation to carbon dioxide (formate → CO_2 = 2e^-) (Table 1). In the case of lactate, ~2.5 moles of Fe(II) was produced per mole of lactate consumed, which is substantially less than 4 moles of Fe(II) per mole of lactate based on the oxidation of lactate to acetate and carbon dioxide (lactate → acetate + CO_2 = 4e^-). In addition, the accumulation of acetate was less than expected based on the amount of lactate consumed (Table 1). Acetate is not used by *S. putrefaciens* CN32 as an electron donor for DIR, but it may have used some acetate as a C source (as could a portion of the lactate consumed).

Compared with formate and lactate, the anaerobic metabolism of pyruvate by *Shewanella* spp. is more complex. In addition to serving as an electron donor for DIR [52,53,71,72,74,75], several *Shewanella* spp. are reported to ferment pyruvate. Fermentation of pyruvate by *Shewanella oneidensis* MR-1 produces acetate, lactate, formate, and H_2 [78] and fermentation by *Shewanella profunda* produces acetate, lactate, and succinate [79]. *S. putrefaciens* ATCC 8071 (formerly *Alteromonas putrefaciens*) used pyruvate as an electron donor for DIR resulting in oxidation to acetate and carbon dioxide (pyruvate → acetate + CO_2 = 2e^-) and stoichiometric production of Fe(II) [72]. However, pyruvate utilization by *S. putrefaciens* W3-18-1 in the presence of Fe(III) oxide likely involved fermentation of pyruvate, and use of pyruvate and pyruvate fermentation products (e.g., formate) as electron donors for DIR [53]. Our results suggest that a similar dynamic occurred with *S. putrefaciens* CN32 in our experimental systems containing pyruvate; if pyruvate was only utilized as an electron donor for DIR, only 30 mM would be needed to account for the ~60 mM of Fe(II) produced, yet all of the pyruvate (75 mM) was consumed.

Few studies have explicitly examined individual amino acids as potential electron donors for anaerobic respiration. Serine, cysteine, glutamate, and aspartate are effective electron donors for anaerobic respiration by *Alteromonas (Shewanllla) putrefaciens* NCMB 1735 using trimethylamine oxide as the terminal electron acceptor [80]. *Geovibrio ferrireducens* can grow by coupling the oxidation of proline to the reduction of Fe(III) [6]. However, none of the amino acids tested by Lovley et al. [15] (glutamine, serine, arginine, leucine, proline, glutamate, tryptophan, and tyrosine) were used as electron donors for DIR by *Geobacter metallireducens*. Among the amino acids examined in this study (alanine, glutamate, glycine, and serine), only serine was an effective electron donor for DIR by *S. putrefaciens* CN32. We did not measure serine concentrations, but serine is easily converted to pyruvate, and pyruvate was observed as a transient intermediate during Fe(III) reduction. Moreover, the Fe(II) production rates in the serine-amended systems were only slightly slower than the rates in the pyruvate-amended systems (which had the fastest rates among the donors tested (Table 1)), consistent with conversion of serine to pyruvate and its subsequent utilization. This is the first report of serine serving as an electron donor for DIR.

NAG is a monomer of chitin, which is present in the cell walls of fungi and the cuticles and exoskeletons of arthropods, mollusks, and worms and is the second most abundant polymer in nature after cellulose. NAG is also a component of cell wall peptidoglycan in gram-positive and gram-negative bacteria. As a product of the microbial decomposition of chitin and peptidoglycan [81,82], NAG is an important component of the organic nitrogen pool in aquatic and terrestrial systems [83–85]. As both a C and N source, NAG is metabolized by a broad range of bacteria [84,86,87]. Many *Shewanella* spp. (including *S. putrefaciens* CN32) respire NAG aerobically [88,89] and several are able to use NAG as a substrate for fermentative growth [88,90,91]. Our study provides the first evidence that a *Shewanella* sp. can use NAG as an electron donor for DIR, an ability that has only been reported for *Thermincola ferriacetica* [92]. The production of Fe(II) was concurrent with NAG consumption and acetate production, which is consistent with NAG serving as an electron donor for Fe(III) reduction. NAG was not consumed independent of Fe(III) reduction suggesting that *S. putrefaciens* CN32 does not ferment NAG.

4.2. Fe(II) Secondary Mineral Formation

The presence of specific electron donors has been shown to have significant impacts on the development of microbial communities and the formation of Fe(II)-bearing minerals in laboratory based-experiments and in-situ studies in subsurface environments [52,53,93–96]. Likewise, in this

study we observe that specific electrons donors lead to the formation specific Fe(II)-bearing secondary minerals during DIR of lepidocrocite by *S. putrefaciens* CN32.

Previous studies of the bioreduction of lepidocrocite have reported magnetite, siderite, vivianite, green rust, and chukanovite as Fe(II)-bearing secondary minerals, with the formation of specific phases attributed to several factors including the rate and extent of Fe(II) production, electron shuttles, the cell number, the extent of particle aggregation, and the presence of sorbates (e.g., oxyanions and DOC) [16,34,41,43–45,49,55,63,97–99]. Stoichiometric conversion to magnetite is often observed during the bioreduction of lepidocrocite [41,44,45,49,63,98]. However, magnetite was not observed as a secondary mineral in any of our experimental systems, likely due to trace levels of phosphate present in the lepidocrocite used in our experiments [63], as low levels of phosphate are known to suppress magnetite formation during DIR of Fe(III) oxides [28,33,44,47,63]. Vivianite formation requires the presence of substantial phosphate (e.g., vivianite was not observed at P:Fe rations lower than 0.08 [33,43,48,63]), and vivianite was not observed in any of our experimental systems (P:Fe = 0.005 [63]). Chukanovite (ferrous hydroxy carbonate) was also not observed in any of our experimental systems. Chukanovite can perhaps be better described as a tertiary product of the DIR of Fe(III) oxides in that it is not observed as an initial product of Fe(III) oxide bioreduction, rather it forms later as a product of the reduction of Fe(II)/Fe(III) secondary minerals like magnetite and green rust [28,37,41,44,49,63,100], and there may not have been sufficient time for chukanovite to form in our experimental systems.

Green rusts were observed as products of lepidocrocite bioreduction by *S. putrefaciens* CN32 when H_2, formate, lactate, or NAG were provided as electron donors (Table 3). Green rusts are layered Fe(II)-Fe(III) hydroxides having a pyroaurite-type structure—i.e., alternating positively charged Fe(II)-Fe(III) hydroxide layers and hydrated anion layers having the general composition: $[Fe^{II}_4\ Fe^{III}_2\ (OH)_{12}]^{2+}\ [(A)_{2/n}\ yH_2O]^{2-}$, where A is an n-valent anion (e.g., Cl^-, SO_4^{2-}, or CO_3^{2-}) and y denotes varying amounts of interlayer water (y = 2 to 4). They are found in Fe(II)-Fe(III) transition zones in a variety of aquatic and terrestrial environments including groundwater [101,102], surface waters [103], soils [104–108], and sediments [109–111], where green rust minerals such as fougérite, trébeurdenite, and mössbauerite [112–114] may play a central role in Fe redox cycling. Green rusts have been reported as secondary mineralization products of the bioreduction of Fe(III) oxides in laboratory-based studies under a wide range of experimental conditions [16,33–35,39,41,44–50,53,55,76,97,100,115–119]. Both carbonate and sulfate green rusts formed depending on the anionic composition of our experimental systems. Carbonate green rust formed in chloride-amended systems, consistent with the affinity of pyroaurite-type layered double hydroxides for carbonate in the interlayer relative to chloride [120]. Furthermore, the production of Fe(II) is coupled to the formation of carbonate from the oxidation of organic electron donors, allowing for carbonate green rust precipitation. Like carbonate, sulfate is preferred over chloride as an interlayer anion in green rusts; as such sulfate green rust formed in our sulfate-amended systems. However, as carbonate accumulates from the oxidation of the organic electron donors, carbonate green rust forms as carbonate is preferred over sulfate in the interlayer. Only carbonate green rust remained in the formate/sulfate system, however both carbonate and sulfate green rusts remained in the lactate/sulfate, and NAG/sulfate systems, likely due to lower carbonate production in those systems.

Siderite ($FeCO_3$) is a geologically significant iron carbonate mineral that is of commercial interest due to its use as a minor iron ore. Siderite is commonly reported as a secondary mineral during the bioreduction of Fe(III) oxides in systems with substantial carbonate concentrations (i.e., >20 mM) [9,33,36,121–123]. In our experimental systems, siderite was observed as the sole secondary mineral in pyruvate-and serine-amended systems (note, as discussed above, serine is likely converted to pyruvate by *S. putrefaciens* CN32). Siderite was also the sole secondary mineral formed during the bioreduction of ferrihydrite and akaganeite by *Shewanella* sp. HN-41 and *S. putrefaciens* W3-18-1, respectively, with pyruvate as the electron donor [52,53]. Although we were not able to measure carbonate concentrations in our experimental systems, it is likely that the use of pyruvate (and serine) as an electron donor results in production of >30 mM given the accumulation of ~60 mM Fe(II) and the

formation of 1 mole of carbonate per 2 moles of Fe(III) reduced based on the oxidation of pyruvate to acetate and carbon dioxide.

In our experimental systems we typically observed formation of either green rust or siderite, except in the NAG-amended systems, where green rust and a minor amount of siderite (<30% of Fe(II)) were observed. Geochemical modeling indicates that pH and carbonate concentration are the key factors determining the prevalence of carbonate green rust verses siderite (Figure 15); ferrous hydroxide and chukanovite were considered in the modeling even though neither were observed in any of our experimental systems. At $a[HCO_3^-] = 10^{-6}$, siderite is not stable. With increasing $a[HCO_3^-]$ the stability field of siderite increases and the stability fields of carbonate green rust and ferrous hydroxide shift to higher pH. These results are consistent with the observed distribution of carbonate green rusts in systems with electron donors likely to result in lower carbonate concentrations (formate, lactate, and NAG) and siderite in systems likely to produce high carbonate concentrations (pyruvate and serine).

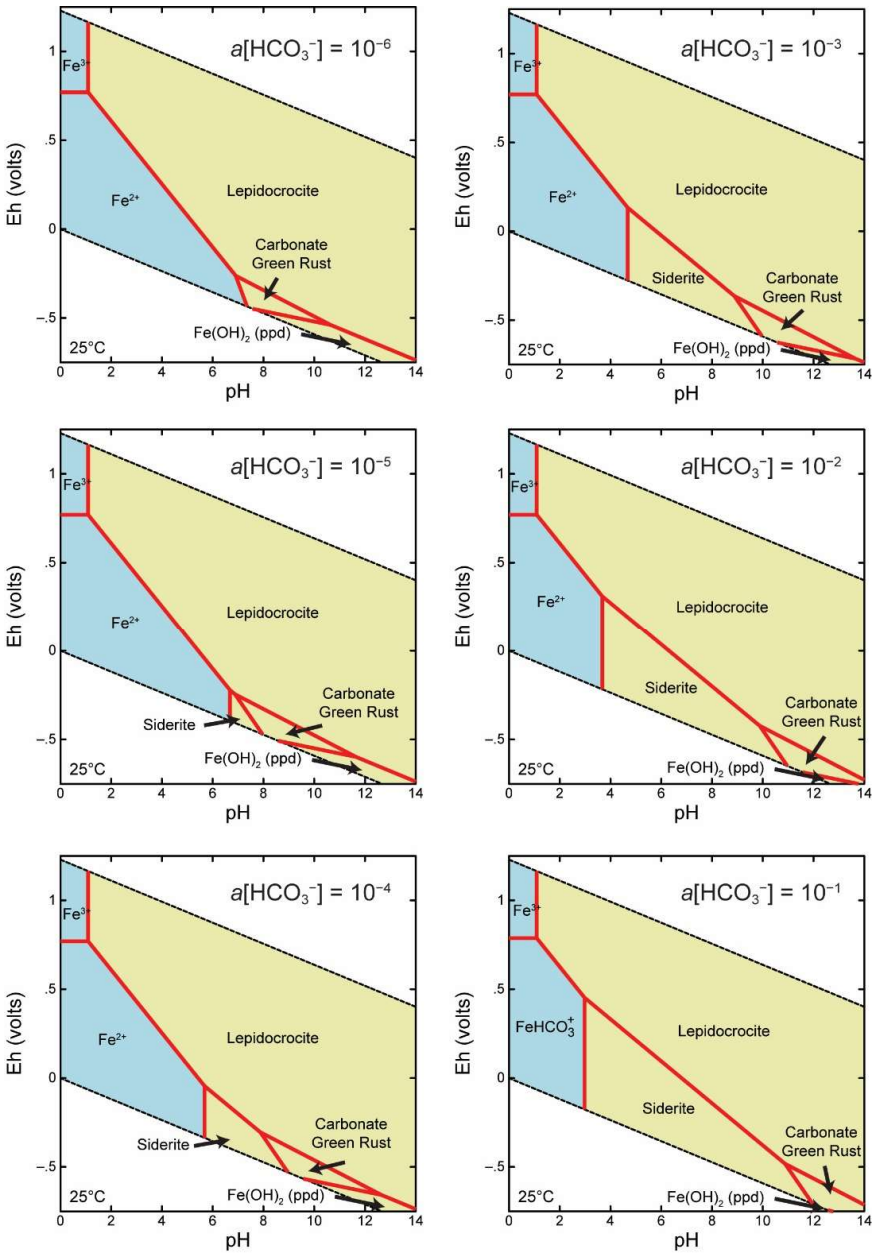

Figure 15. Eh-pH diagrams of iron ($a[Fe^{2+}] = 10^{-3}$) in aqueous solution containing dissolved carbonate ranging from $a[HCO_3^-] = 10^{-6}$–10^{-1} at 30 °C.

4.3. Environmental Relevance

Largely through the activity of DIRB, Fe(II) is typically one of the most abundant reductants present in aquatic and terrestrial environments under suboxic and anoxic conditions [124–126], often providing substantial redox buffering capacity to these systems. Fe(II) is a reductant for a wide range of contaminants, however, the redox reactivity of Fe(II) depends strongly on its speciation [127–131]. Among the Fe(II)-bearing secondary minerals resulting from DIR of Fe(III) oxides, green rusts are a particularly effective reductant for a wide range of contaminants of concern, including chlorinated solvents, nitroaromatics, azo dyes, toxic metals, metallolids, and radionuclides [127,128,132–153]. Therefore, identifying the factors (e.g., availability of specific electron donors) that lead to the formation of green rusts and other reactive Fe(II) phases in natural and engineered environments may lead to better management of contaminant fate and transport (e.g., in situ biostimulation of DIRB for contaminant bioremediation).

Author Contributions: E.J.O. initiated the concept and carried out the experiments. C.A.G. and M.M.S. performed the ^{57}Fe Mössbauer analysis. T.M.F. performed the geochemical modeling. E.J.O. drafted the manuscript and all authors reviewed and edited the final version.

Funding: This research is part of the Subsurface Science Scientific Focus Area (SFA) at Argonne National Laboratory supported by the Subsurface Biogeochemical Research Program, Office of the Biological and Environmental Research, Office of Science, U.S. Department of Energy (DOE), under contract DE-AC02-06CH11357. This work was performed, in part, at the Center for Nanoscale Materials, a U.S. Department of Energy Office of Science User Facility, and supported by the U.S. Department of Energy, Office of Science, under Contract No. DE-AC02-06CH11357.

Acknowledgments: We thank Russell Cook for his assistance with SEM imaging and two anonymous reviewers for their thoughtful reviews of the manuscript.

Conflicts of Interest: The authors declare no conflict of interest. The funders had no role in the design of the study; in the collection, analyses, or interpretation of data; in the writing of the manuscript, or in the decision to publish the results.

References

1. Canfield, D.E.; Thamdrup, B.; Hansen, J.W. The anaerobic degradation of organic matter in Danish coastal sediments: Iron reduction, manganese reduction, and sulfate reduction. *Geochim. Cosmochim. Acta* **1993**, *57*, 3867–3883. [CrossRef]
2. Nealson, K.H.; Saffarini, D.A. Iron and manganese in anaerobic respiration: Environmental significance, physiology, and regulation. *Annu. Rev. Microbiol.* **1994**, *48*, 311–343. [CrossRef] [PubMed]
3. Roden, E.E.; Wetzel, R.G. Organic carbon oxidation and methane production by microbial Fe(III) oxide reduction in vegetated and unvegetated freshwater wetland sediments. *Limnol. Oceanogr.* **1996**, *41*, 1733–1748. [CrossRef]
4. Lovley, D.R. Fe(III) and Mn(IV) reduction. In *Environmental Microbe-Metal Interactions*; Lovley, D.R., Ed.; American Society for Microbiology Press: Washington, DC, USA, 2000; pp. 3–30.
5. Thamdrup, B. Bacterial manganese and iron reduction in aquatic sediments. *Adv. Microb. Ecol.* **2000**, *16*, 41–84.
6. Caccavo, F., Jr.; Coates, J.D.; Rossello-Mora, R.A.; Ludwig, W.; Schleifer, K.H.; Lovley, D.R.; McInerney, M.J. *Geovibrio ferrireducens*, a phylogenetically distinct dissimilatory Fe(III)-reducing bacterium. *Arch. Microbiol.* **1996**, *165*, 370–376. [CrossRef] [PubMed]
7. Coates, J.D.; Bhupathiraju, V.K.; Achenbach, L.; McInerney, M.J.; Lovley, D.R. *Geobacter hydrogenophilus*, *Geobacter chapelli* and *Geobacter grbiciae*, three new, strictly anaerobic, dissimilatory Fe(III)-reducers. *Int. J. Syst. Evol. Microbiol.* **2001**, *51*, 581–588. [CrossRef] [PubMed]
8. Coates, J.D.; Ellis, D.J.; Gaw, C.V.; Lovley, D.R. *Geothrix fermentans* gen. nov., sp. nov., a novel Fe(III)-reducing bacterium from a hydrocarbon-contaminated aquifer. *Int. J. Syst. Bacteriol.* **1999**, *49*, 1615–1622. [CrossRef]
9. Dong, Y.; Sanford, R.A.; Boyanov, M.I.; Kemner, K.M.; Flynn, T.M.; O'Loughlin, E.J.; Chang, Y.J.; Locke, R.A., Jr.; Weber, J.R.; Egan, S.M.; et al. *Orenia metallireducens* sp. nov. strain Z6, a novel metal-reducing member of the phylum firmicutes from the deep subsurface. *Appl. Environ. Microbiol.* **2016**, *82*, 6440–6453. [CrossRef]

10. Dong, Y.; Sanford, R.A.; Boyanov, M.I.; Kemner, K.M.; Flynn, T.M.; O'Loughlin, E.J.; Locke Ii, R.A.; Weber, J.R.; Egan, S.M.; Fouke, B.W. *Tepidibacillus decaturensis* sp. nov.: A microaerophilic, moderately thermophilic iron-reducing bacterium isolated from a depth of 1.7 km in the Illinois Basin, USA. *Int. J. Syst. Evol. Microbiol.* **2016**. [CrossRef]
11. Ettwig, K.F.; Zhu, B.; Speth, D.; Keltjens, J.T.; Jetten, M.S.; Kartal, B. Archaea catalyze iron-dependent anaerobic oxidation of methane. *Proc. Natl. Acad. Sci. USA* **2016**. [CrossRef]
12. Kashefi, K.; Lovley, D.R. Reduction of Fe(III), Mn(IV), and toxic metals at 100 °C by *Pyrobacterium islandicum*. *Appl. Environ. Microbiol.* **2000**, *66*, 1050–1056. [CrossRef] [PubMed]
13. Sanford, R.A.; Cole, J.R.; Tiedje, J.M. Characterization and description of *Anaeromyxobacter dehalogens* gen. nov., sp. nov., an Aryl-halorespiring facultative anaerobic myxobacterium. *Appl. Environ. Microbiol.* **2002**, *68*, 893–900. [CrossRef] [PubMed]
14. Roh, Y.; Liu, S.V.; Li, G.; Huang, H.; Phelps, T.J.; Zhou, J. Isolation and characterization of metal-reducing *Thermoanaerobacter* strains from deep subsurface environments of the Piceance Basin, Colorado. *Appl. Environ. Microbiol.* **2002**, *68*, 6013–6020. [CrossRef] [PubMed]
15. Lovley, D.R.; Giovanoli, S.J.; White, D.C.; Champine, J.E.; Phillips, E.J.P.; Gorby, Y.A.; Goodwin, S. *Geobacter metallireducens* gen. nov. sp. nov., a microorganism capable of coupling the complete oxidation of organic compounds to the reduction of iron and other metals. *Arch. Microbiol.* **1993**, *159*, 336–344. [CrossRef] [PubMed]
16. O'Loughlin, E.J.; Larese-Casanova, P.; Scherer, M.M.; Cook, R.E. Green rust formation from the bioreduction of g-FeOOH (lepidocrocite): Comparison of several *Shewanella* species. *Geomicrobiol. J.* **2007**, *24*, 211–230. [CrossRef]
17. Slobodkin, A.; Reysenbach, A.L.; Strutz, N.; Dreier, M.; Wiegel, J. *Thermoterrabacterium ferrireducens* gen. nov., sp. nov., a thermophilic anaerobic dissimilatory Fe(III)-reducing bacterium from a continental hot spring. *Int. J. Syst. Bacteriol.* **1997**, *47*, 541–547. [CrossRef] [PubMed]
18. Greene, A.C.; Patel, B.K.; Sheehy, A.J. Deferribacter thermophilus gen. nov., sp. nov., a novel thermophilic manganese- and iron-reducing bacterium isolated from a petroleum reservoir. *Int. J. Syst. Bacteriol.* **1997**, *47*, 505–509. [CrossRef] [PubMed]
19. Roh, Y.; Chon, C.-M.; Moon, J.-W. Metal reduction and biomineralization by an alkaliphilic metal-reducing bacterium, *Alkaliphilus metalliredigens* (QYMF). *Geosci. J.* **2007**, *11*, 415–423. [CrossRef]
20. Cutting, R.S.; Coker, V.S.; Fellowes, J.W.; Lloyd, J.R.; Vaughan, D.J. Mineralogical and morphological constraints on the reduction of Fe(III) minerals by *Geobacter sulfurreducens*. *Geochim. Cosmochim. Acta* **2009**, *73*, 4004–4022. [CrossRef]
21. Shelobolina, E.S.; Vanpraagh, C.G.; Lovley, D.R. Use of ferric and ferrous iron containing minerals for respiration by *Desulfitobacterium frappieri*. *Geomicrobiol. J.* **2003**, *20*, 143–156. [CrossRef]
22. Kostka, J.E.; Haefele, E.; Viehweger, R.; Stucki, J.W. Respiration and dissolution of iron(III)-containing clay minerals by bacteria. *Environ. Sci. Technol.* **1999**, *33*, 3127–3133. [CrossRef]
23. Kostka, J.E.; Nealson, K.H. Dissolution and reduction of magnetite by bacteria. *Environ. Sci. Technol.* **1995**, *29*, 2535–2540. [CrossRef] [PubMed]
24. Urrutia, M.M.; Roden, E.E.; Fredrickson, J.K.; Zachara, J.M. Microbial and surface chemistry controls on reduction of synthetic Fe(III) oxide minerals by the dissimilatory iron-reducing bacterium *Shewanella alga*. *Geomicrobiology* **1998**, *15*, 269–291. [CrossRef]
25. Zachara, J.M.; Fredrickson, J.K.; Li, S.-M.; Kennedy, D.W.; Smith, S.C.; Gassman, P.L. Bacterial reduction of crystalline Fe^{3+} oxides in single phase suspension and subsurface materials. *Am. Mineral.* **1998**, *83*, 1426–1443. [CrossRef]
26. Lee, S.H.; Lee, I.; Roh, Y. Biomineralization of a poorly crystalline Fe(III) oxide, akaganeite, by an anaerobic Fe(III)-reducing bacterium (*Shewanella alga*) isolated from marine environment. *Geosci. J.* **2003**, *7*, 217–226. [CrossRef]
27. Seabaugh, J.L.; Dong, H.; Kukkadapu, R.K.; Eberl, D.D.; Morton, J.P.; Kim, J. Microbial reduction of Fe(III) in the Fithian and Muloorina illites: Contrasting extents and rates of bioreduction. *Clays Clay Miner.* **2006**, *54*, 67–79. [CrossRef]
28. O'Loughlin, E.J.; Gorski, C.A.; Scherer, M.M. Effects of phosphate on secondary mineral formation during the bioreduction of akaganeite (b-FeOOH): Green rust versus framboidal magnetite. *Curr. Inorg. Chem.* **2015**, *5*, 214–224. [CrossRef]

29. Thurman, E.M. *Organic Geochemistry of Natural Waters*; Martinus Nijhoff/Dr. W. Junk Publishers: Dordrecht, The Netherlands, 1985; p. 497.
30. Megonigal, J.P.; Hines, M.E.; Visscher, P.T. Anaerobic metabolism: Linkages to trace gasses and aerobic processes. In *Biogeochemistry*; Schlesinger, W.H., Ed.; Elsevier-Pergamon: Oxford, UK, 2004; pp. 317–424.
31. Lovley, D.R. Microbial Fe(III) reduction in subsurface environments. *FEMS Microbiol. Rev.* **1997**, *20*, 305–313. [CrossRef]
32. Lovley, D.R.; Stolz, J.F.; Nord, G.L., Jr.; Phillips, E.J.P. Anaerobic production of magnetite by a dissimilatory iron-reducing microorganism. *Nature* **1987**, *330*, 252–254. [CrossRef]
33. Fredrickson, J.K.; Zachara, J.M.; Kennedy, D.W.; Dong, H.; Onstott, T.C.; Hinman, N.W.; Li, S.-M. Biogenic iron mineralization accompanying the dissimilatory reduction of hydrous ferric oxide by a groundwater bacterium. *Geochim. Cosmochim. Acta* **1998**, *62*, 3239–3257. [CrossRef]
34. Ona-Nguema, G.; Abdelmoula, M.; Jorand, F.; Benali, O.; Géhin, A.; Block, J.-C.; Génin, J.-M.R. Iron(II,III) hydroxycarbonate green rust formation and stabilization from lepidocrocite bioreduction. *Environ. Sci. Technol.* **2002**, *36*, 16–20. [CrossRef] [PubMed]
35. Glasauer, S.; Weidler, P.G.; Langley, S.; Beveridge, T.J. Controls on Fe reduction and mineral formation by a subsurface bacterium. *Geochim. Cosmochim. Acta* **2003**, *67*, 1277–1288. [CrossRef]
36. Roh, Y.; Zhang, C.-L.; Vali, H.; Lauf, R.J.; Zhou, J.; Phelps, T.J. Biogeochemical and environmental factors in Fe biomineralization: Magnetite and siderite formation. *Clays Clay Miner.* **2003**, *51*, 83–95. [CrossRef]
37. Kukkadapu, R.K.; Zachara, J.M.; Fredrickson, J.K.; Kennedy, D.W.; Dohnalkova, A.C.; Mccready, D.E. Ferrous hydroxy carbonate is a stable transformation product of biogenic magnetite. *Am. Mineral.* **2005**, *90*, 510–515. [CrossRef]
38. Behrends, T.; Van Cappellen, P. Transformation of hematite into magnetite during dissimilatory iron reduction-conditions and mechanisms. *Geomicrobiol. J.* **2007**, *24*, 403–416. [CrossRef]
39. Boyanov, M.I.; O'Loughlin, E.J.; Kemner, K.M. Iron phase transformations resulting from the respiration of *Shewanella putrefaciens* on a mixed mineral phase. *J. Phys. Conf. Ser.* **2009**, *190*, 012193. [CrossRef]
40. Shelobolina, E.; Konishi, H.; Xu, H.; Benzine, J.; Xiong, M.Y.; Wu, T.; Blothe, M.; Roden, E. Isolation of phyllosilicate-iron redox cycling microorganisms from an illite-smectite rich hydromorphic soil. *Front. Microbiol.* **2012**, *3*, 134. [CrossRef]
41. Zegeye, A.; Mustin, C.; Jorand, F. Bacterial and iron oxide aggregates mediate secondary iron mineral formation: Green rust versus magnetite. *Geobiology* **2010**, *8*, 209–222. [CrossRef]
42. Zachara, J.M.; Kukkadapu, R.K.; Frederickson, J.K.; Gorby, Y.A.; Smith, S.C. Biomineralization of poorly crystalline Fe(III) oxides by dissimilatory metal reducing bacteria (DMRB). *Geomicrobiol. J.* **2002**, *19*, 179–207. [CrossRef]
43. Bae, S.; Lee, W. Biotransformation of lepidocrocite in the presence of quinones and flavins. *Geochim. Cosmochim. Acta* **2013**, 10. [CrossRef]
44. O'Loughlin, E.J.; Gorski, C.; Scherer, M.M.; Boyanov, M.I.; Kemner, K.M. Effects of oxyanions, natural organic matter, and cell density on the bioreduction of lepidocrocite (g-FeOOH) and secondary mineral formation. *Environ. Sci. Technol.* **2010**, *44*, 4570–4576. [CrossRef] [PubMed]
45. Zegeye, A.; Ruby, C.; Jorand, F. Kinetic and thermodynamic analysis during dissimilatory g-FeOOH reduction: Formation of green rust 1 and magnetite. *Geomicrobiol. J.* **2007**, *24*, 51–64. [CrossRef]
46. Salas, E.C.; Berelson, W.M.; Hammond, D.E.; Kampf, A.R.; Nealson, K.H. The impact of bacterial strain on the products of dissimilatory iron reduction. *Geochim. Cosmochim. Acta* **2010**, *74*, 574–583. [CrossRef] [PubMed]
47. Borch, T.; Masue, Y.; Kukkadapu, R.K.; Fendorf, S. Phosphate imposed limitations on biological reduction and alteration of ferrihydrite. *Environ. Sci. Technol.* **2007**, *41*, 166–172. [CrossRef] [PubMed]
48. Kukkadapu, R.K.; Zachara, J.M.; Fredrickson, J.K.; Kennedy, D.W. Biotransformation of two-line silica-ferrihydrite by a dissimilatory Fe(III)-reducing bacterium: Formation of carbonate green rust in the presence of phosphate. *Geochim. Cosmochim. Acta* **2004**, *68*, 2799–2814. [CrossRef]
49. Sergent, A.-S.; Jorand, F.; Hanna, K. Effects of Si-bearing minerals on the nature of secondary iron mineral products from lepidocrocite bioreduction. *Chem. Geol.* **2011**, *289*, 86–97. [CrossRef]
50. Jorand, F.; Zegeye, A.; Ghanbaja, J.; Abdelmoula, M. The formation of green rust induced by tropical river biofilm components. *Sci. Total Envrion.* **2011**, *409*, 2586–2596. [CrossRef]
51. Fredrickson, J.K.; Kota, S.; Kukkadapu, R.K.; Liu, C.; Zachara, J.M. Influence of electron donor/acceptor concentrations on hydrous ferric oxide (HFO) bioreduction. *Biodegradation* **2003**, *14*, 91–103. [CrossRef]

52. Lee, J.-H.; Roh, Y.; Kim, K.-W.; Hur, H.-G. Organic acid-dependent iron mineral formation by a newly isolated iron-reducing bacterium, *Shewanella* sp. HN-41. *Geomicrobiol. J.* **2007**, *24*, 31–41. [CrossRef]
53. Salas, E.C.; Berelson, W.M.; Hammond, D.E.; Kampf, A.R.; Nealson, K.H. The influence of carbon source on the products of dissimilatory iron reduction. *Geomicrobiol. J.* **2009**, *26*, 451–462. [CrossRef]
54. Lovley, D. Dissimilatory Fe(III)- and Mn(IV)-reducing prokaryotes. In *The Prokaryotes—Prokaryotic Physiology and Biochemistry*; Dworkin, M., Ed.; Springer: Berlin/Heidelburg, Germany, 2013; pp. 287–308.
55. O'Loughlin, E.J. Effects of electron transfer mediators on the biodegradation of lepidocrocite (g-FeOOH) by *Shewanella putrefaciens* CN32. *Environ. Sci. Technol.* **2008**, *42*, 6876–6882. [CrossRef] [PubMed]
56. Stookey, L.L. Ferrozine-A new spectrophotometric reagent for iron. *Anal. Chem.* **1970**, *42*, 779–781. [CrossRef]
57. Sørensen, J. Reduction of ferric iron in anaerobic, marine sediment and interaction with reduction of nitrate and sulfate. *Appl. Environ. Microbiol.* **1982**, *43*, 319–324. [PubMed]
58. Bethke, C.M. *Geochemical and Biogeochemical Reaction Modelling*, 2nd ed.; Cambridge University Press: Cambridge, UK, 2008; p. 543.
59. Delany, J.M.; Lundeen, S.R. *The LLNL Thermochemical Database*; Lawrence Livermore National Laboratory: Livermore, CA, USA, 1989; Report UCRL-21658; p. 150.
60. Allison, J.D.; Brown, D.S.; Novo-Gradac, K.J. *MINTEQA2/PRODEFA2, A Geochemical Assessment Model for Environmental Systems: Version 3.0 User's Manual*; USEPA: Washington, DC, USA, 1991.
61. Drissi, S.H.; Refait, P.; Abdelmoula, M.; Génin, J.M.R. The preparation and thermodynamic properties of Fe(II)-Fe(III) hydroxide-carbonate (green rust 1); Pourbaix diagram of iron in carbonate-containing aqueous media. *Corros. Sci.* **1995**, *37*, 2025–2041. [CrossRef]
62. Azoulay, I.; Rémazeilles, C.; Refait, P. Determination of standard Gibbs free energy of formation of chukanovite and Pourbaix diagrams of iron in carbonated media. *Corros. Sci.* **2012**, *58*, 229–236. [CrossRef]
63. O'Loughlin, E.J.; Boyanov, M.I.; Flynn, T.M.; Gorski, C.; Hofmann, S.M.; McCormick, M.L.; Scherer, M.M.; Kemner, K.M. Effects of bound phosphate on the bioreduction of lepidocrocite (g-FeOOH) and maghemite (g-Fe_2O_3) and formation of secondary minerals. *Environ. Sci. Technol.* **2013**, *47*, 9157–9166. [CrossRef]
64. Hau, H.H.; Gralnick, J.A. Ecology and biotechnology of the genus *Shewanella*. *Annu. Rev. Microbiol.* **2007**, *61*, 237–258. [CrossRef] [PubMed]
65. Fredrickson, J.K.; Romine, M.F.; Beliaev, A.S.; Auchtung, J.M.; Driscoll, M.E.; Gardner, T.S.; Nealson, K.H.; Osterman, A.L.; Pinchuk, G.; Reed, J.L.; et al. Towards environmental systems biology of *Shewanella*. *Nat. Rev. Microbiol.* **2008**, *6*, 592–603. [CrossRef] [PubMed]
66. Janda, J.M.; Abbott, S.L. The genus *Shewanella*: From the briny depths below to human pathogen. *Crit. Rev. Microbiol.* **2014**, *40*, 293–312. [CrossRef]
67. Serres, M.H.; Riley, M. Genomic analysis of carbon source metabolism of *Shewanella oneidensis* MR-1: Predictions versus experiments. *J. Bacteriol.* **2006**, *188*, 4601–4609. [CrossRef]
68. Pinchuk, G.; Hill, E.A.; Geydebrekht, O.V.; De Ingeniis, J.; Zhang, X.; Osterman, A.; Scott, J.H.; Reed, S.B.; Romine, M.F.; Konopka, A.E.; et al. Constraint-based model of *Shewanella oneidensis* MR-1 metabolism: A tool for data analysis and hypothesis generation. *PLoS Comput. Biol.* **2010**, *6*, e1000822. [CrossRef] [PubMed]
69. Rodionov, D.A.; Yang, C.; Li, X.; Rodionova, I.A.; Wang, Y.; Obraztsova, A.Y.; Zagnitko, O.P.; Overbeek, R.; Romine, M.F.; Reed, S.; et al. Genomic encyclopedia of sugar utilization pathways in the Shewanella genus. *BMC Genom.* **2010**, *11*, 494. [CrossRef]
70. Nealson, K.H.; Scott, J. Ecophysiology of the genus *Shewanella*. In *The Prokaryotes: An Evolving Electronic Resource for the Microbiological Community*; Dworkin, M., Ed.; Springer: New York, NY, USA, 2006; Volume 6, pp. 848–860.
71. Caccavo, F., Jr.; Blakemore, R.P.; Lovley, D.R. A hydrogen-oxidizing, Fe(III)-reducing microorganism from the Great Bay Estuary, New Hampshire. *Appl. Environ. Microbiol.* **1992**, *58*, 3211–3216. [PubMed]
72. Lovley, D.R.; Phillips, E.J.P.; Lonergan, D.J. Hydrogen and formate oxidation coupled to dissimilatory reduction of iron or manganese by *Alteromonas putrefaciens*. *Appl. Environ. Microbiol.* **1989**, *55*, 700–706. [PubMed]
73. Liu, C.; Gorby, Y.A.; Zachara, J.M.; Fredrickson, J.K.; Brown, C.F. Reduction kinetics of Fe(III), Co(III), U(VI), Cr(VI), and Tc(VII) in cultures of dissimilatory metal-reducing bacteria. *Biotechnol. Bioeng.* **2002**, *80*, 637–649. [CrossRef] [PubMed]

74. Stapleton, R.D.; Sabree, Z.L.; Palumbo, A.V.; Moyer, C.L.; Devol, A.H.; Roh, Y.; Zhou, J. Metal reduction at cold temperatures by *Shewanella* isolates from various marine environments. *Aquat. Microb. Ecol.* **2005**, *38*, 81–91. [CrossRef]
75. Roh, Y.; Gao, H.; Vali, H.; Kennedy, D.W.; Yang, Z.K.; Gao, W.; Dohnalkova, A.C.; Stapleton, R.D.; Moon, J.-W.; Phelps, T.J.; et al. Metal reduction and iron biomineralization by a psychrotolerant Fe(III)-reducing bacterium, *Shewanella* sp. strain PV-4. *Appl. Environ. Microbiol.* **2006**, *72*, 3236–3244. [CrossRef]
76. Zegeye, A.; Ona-Nguema, G.; Carteret, C.; Huguet, L.; Abdelmoula, M.; Jorand, F. Formation of hydroxysulfate green rust 2 as a single iron(II-III) mineral in microbial culture. *Geomicrobiol. J.* **2005**, *22*, 389–399. [CrossRef]
77. Jorand, F.P.A.; Sergent, A.S.; Remy, P.P.; Bihannic, I.; Ghanbaja, J.; Lartiges, B.; Hanna, K.; Zegeye, A. Contribution of anionic vs. neutral polymers to the formation of green rust 1 from γ-FeOOH bioreduction. *Geomicrobiol. J.* **2013**, *30*, 600–615. [CrossRef]
78. Pinchuk, G.E.; Geydebrekht, O.V.; Hill, E.A.; Reed, J.L.; Konopka, A.E.; Beliaev, A.S.; Fredrickson, J.K. Pyruvate and lactate metabolism by *Shewanella oneidensis* MR-1 under fermentation, oxygen limitation, and fumarate respiration conditions. *Appl. Environ. Microbiol.* **2011**, *77*, 8234–8240. [CrossRef]
79. Toffin, L.; Bidault, A.; Pignet, P.; Tindall, B.J.; Slobodkin, A.; Kato, C.; Prieur, D. *Shewanella profunda* sp. nov., isolated from deep marine sediment of the Nanki Trough. *Int. J. Syst. Evol. Microbiol.* **2004**, *54*, 1943–1949. [CrossRef] [PubMed]
80. Ringø, E.; Stenberg, E.; Strøm, A.R. Amino acid and lactate catabolism in trimethylamine oxide respiration of *Alteromonas putrefaciens* NCMB 1735. *Appl. Environ. Microbiol.* **1984**, *46*, 1084–1089.
81. Jørgensen, N.O.G.; Stepanaukas, R.; Pedersen, A.-G.U.; Hansen, M.; Nybroe, O. Occurrence and degradation of peptidoglycan in aquatic environments. *FEMS Microbiol. Ecol.* **2003**, *46*, 269–280. [CrossRef]
82. Beier, S.; Bertilsson, S. Bacterial chitin degradation-mechanisms and ecophysiological strategies. *Front. Microbiol.* **2013**, *4*, 149. [CrossRef] [PubMed]
83. Nedoma, J.; Vrba, J.; Hejzlar, J.; Šimek, K.; Straškrabová, V. N-acetylglucosamine dynamics in freshwater environments: Concentration of amino sugars, extracellular enzyme activities, and microbial uptake. *Limnol. Oceanogr.* **1994**, *39*, 1088–1100. [CrossRef]
84. Riemann, L.; Azam, F. Widespread *N*-acetyl-D-glucosamine uptake among pelagic marine bacteria and its ecological implications. *Appl. Environ. Microbiol.* **2002**, *68*, 5554–5562. [CrossRef] [PubMed]
85. Roberts, P.; Jones, D.L. Microbial and plant uptake of free amino sugars in grassland soils. *Soil Biol. Biochem.* **2012**, *49*, 139–149. [CrossRef]
86. Beier, S.; Bertilsson, S. Uncoupling of chitinase activity and uptake of hydrolysis products in freshwater bacterioplankton. *Limnol. Oceanogr.* **2011**, *56*, 1179–1188. [CrossRef]
87. Tada, Y.; Grossart, H.P. Community shifts of actively growing lake bacteria after N-acetyl-glucosamine addition: Improving the BrdU-FACS method. *ISME J.* **2014**, *8*, 441–454. [CrossRef]
88. Satomi, M.; Oikawa, H.; Yano, Y. *Shewanella marinintestina* sp. nov., *Shewanella schlegeliana* sp. nov. and *Shewanella sairae* sp. nov., novel eicosapentaenoic-acid-producing marine bacteria isolated from sea-animal intestines. *Int. J. Syst. Evol. Microbiol.* **2003**, *53*, 491–499. [CrossRef]
89. Yang, C.; Rodionov, D.A.; Li, X.; Laikova, O.N.; Gelfand, M.S.; Zagnitko, O.P.; Romine, M.F.; Obraztsova, A.Y.; Nealson, K.H.; Osterman, A.L. Comparative genomics and experimental characterization of *N*-acetylglucosamine utilization pathway of *Shewanella oneidensis*. *J. Biol. Chem.* **2006**, *281*, 29872–29885. [CrossRef] [PubMed]
90. Bowman, J.P.; McCammon, S.; Nichols, D.S.; Skerratt, J.H.; Rea, S.M.; Nichols, P.D.; McMeekin, T.A. *Shewanella gelidimarina* sp. nov. and *Shewanella frigidimarina* sp. nov., novel antarctic species with the ability to produce eicosapentaenoic acid (20:5 ω3) and grow anaerobically by dissimilatory Fe(III) reduction. *Int. J. Syst. Bacteriol.* **1997**, *47*, 1040–1047. [CrossRef] [PubMed]
91. Bozal, N.; Montes, M.J.; Tudela, E.; Jimenez, F.; Guinea, J. *Shewanella frigidimarina* and *Shewanella livingstonensis* sp. nov. isolated from Antarctic coastal areas. *Int. J. Syst. Evol. Microbiol.* **2002**, *52*, 195–205. [CrossRef] [PubMed]
92. Zavarzina, D.G.; Sokolova, T.G.; Tourova, T.P.; Chernyh, N.A.; Kostrikina, N.A.; Bonch-Osmolovskaya, E.A. *Thermincola ferriacetica* sp. nov., a new anaerobic, thermophilic, facultatively chemolithoautotrophic bacterium capable of dissimilatory Fe(III) reduction. *Extremeophiles* **2007**, *11*, 1–7. [CrossRef] [PubMed]

93. Akob, D.M.; Mills, H.J.; Gihring, T.M.; Kerkhof, L.; Stucki, J.W.; Anastacio, A.S.; Chin, K.-J.; Kusel, K.; Palumbo, A.V.; Watson, D.B.; et al. Functional diversity and electron donor dependence of microbial populations capable of U(VI) reduction in radionuclide-contaminated subsurface sediments. *Appl. Environ. Microbiol.* **2008**, *74*, 3159–3170. [CrossRef]
94. Lentini, C.J.; Wankel, S.D.; Hansel, C.M. Enriched iron(III)-reducing bacterial communities are shaped by carbon substrate and iron mineralogy. *Front. Microbiol.* **2012**, *3*. [CrossRef] [PubMed]
95. Petrie, L.; North, N.N.; Dollhopf, S.L.; Balkwill, D.L.; Kostka, J.E. Enumeration and characterization of iron(III)-reducing microbial communities and acidic subsurface sediments contaminated with uranium(VI). *Appl. Environ. Microbiol.* **2003**, *69*, 7467–7479. [CrossRef]
96. Kwon, M.J.; O'Loughlin, E.J.; Boyanov, M.I.; Brulc, J.M.; Johnston, E.R.; Kemner, K.M.; Antonopoulos, D.A. Impact of organic carbon electron donors on microbial community development under iron- and sulfate-reducing conditions. *PLoS ONE* **2016**, *11*, 1–22. [CrossRef]
97. Jung, J.; Bae, S.; Lee, W. Indirect contact of bio-transformation of lepidocrocite: Role of electron transfer mediator. *Sustain. Environ. Res.* **2012**, *23*, 193–198.
98. Ona-Nguema, G.; Jorand, F.; Benali, O.; Abdelmoula, M.; Génin, J.-M.R.; Block, J.-C. Key role of the kinetics of g-FeOOH bioreduction on the formation of Fe(II-III) minerals. In *Hyperfine Interactions (C), Proceedings of the International Conference on the Applications of the Mössbauer Effect (ICAME 2001), Oxford, UK, 2–7 September 2001*; Thomas, M.F., Williams, J.M., Gibb, T.C., Eds.; Kluwer Academic Publishers: Dordrecht, The Netherlands, 2002; pp. 415–418.
99. Ona-Nguema, G.; Morin, G.; Juillot, F.; Calas, G.; Brown, G.E., Jr. EXAFS analysis of arsenite adsorption onto two-line ferrihydrite, hematite, goethite, and lepidocrocite. *Environ. Sci. Technol.* **2005**, *39*, 9147–9155. [CrossRef]
100. Ona-Nguema, G.; Morin, G.; Wang, Y.; Menguy, N.; Juillot, F.; Olovi, L.; Aquilanti, G.; Abdelmoula, M.; Ruby, C.; Bargar, J.R.; et al. Arsenite sequestration at the surface of nano-$Fe(OH)_2$, ferrous-carbonate hydroxide, and green-rust after bioreduction of arsenic-sorbed lepidocrocite by *Shewanella putrefaciens*. *Geochim. Cosmochim. Acta* **2009**, *73*, 1359–1381. [CrossRef]
101. Christiansen, B.C.; Balic-Zunic, T.; Dideriksen, K.; Stipp, S.L.S. Identification of green rust in groundwater. *Environ. Sci. Technol.* **2009**, *43*, 3436–3441. [CrossRef] [PubMed]
102. Johnson, C.A.; Freyer, G.; Fabisch, M.; Caraballo, M.A.; Küsel, K.; Hochella, M.F. Observations and assessment of iron oxide and green rust nanoparticles in metal-polluted mine drainage within a steep redox gradient. *Environ. Chem.* **2014**, *11*, 377. [CrossRef]
103. Zegeye, A.; Bonneville, S.; Benning, L.G.; Sturm, A.; Fowle, D.A.; Jones, C.; Canfield, D.E.; Ruby, C.; MacLean, L.C.; Nomosatryo, S.; et al. Green rust formation controls nutrient availability in a ferruginous water column. *Geology* **2012**, *40*, 599–602. [CrossRef]
104. Feder, F.; Trolard, F.; Klingelhöfer, G.; Bourrié, G. In situ Mössbauer spectroscopy: Evidence for green rust (fougerite) in a gleysol and its mineralogical transformations with time and depth. *Geochim. Cosmochim. Acta* **2005**, *69*, 4463–4483. [CrossRef]
105. Génin, J.-M.R.; Bourrié, G.; Trolard, F.; Abdelmoula, M.; Jaffrezic, A.; Refait, P.; Maitre, V.; Humbert, B.; Herbillon, A. Thermodynamic equilibria in aqueous suspensions of synthetic and natural Fe(II)-Fe(III) green rusts: Occurrences of the mineral in hydromorphic soils. *Environ. Sci. Technol.* **1998**, *32*, 1058–1068. [CrossRef]
106. Refait, P.; Abdelmoula, M.; Trolard, F.; Génin, J.-M.R.; Ehrhardt, J.J.; Bourrié, G. Mössbauer and XAS study of a green rust mineral: The partial substitution of Fe^{2+} by Mg^{2+}. *Am. Mineral.* **2001**, *86*, 731–739. [CrossRef]
107. Trolard, F.; Génin, J.-M.R.; Abdelmoula, M.; Bourrié, G.; Humbert, B.; Herbillon, A. Identification of a green rust mineral in a reductomorphic soil by Mössbauer and Raman spectroscopies. *Geochim. Cosmochim. Acta* **1997**, *61*, 1107–1111. [CrossRef]
108. Weatherington-Rice, J.; Bigham, J.M. Buried pre-Illinoian-age lacustrine deposits with "green rust" colors in Clermont County, Ohio. *Ohio J. Sci.* **2006**, *106*, 35–44.
109. Bearcock, J.M.; Perkins, W.T.; Dinelli, E.; Wade, S.C. Fe(II)/Fe(III) "green rust" developed within ocherous coal mine drainage sediment in South Wales, UK. *Mineral. Mag.* **2006**, *70*, 731–741. [CrossRef]
110. Bender Koch, C.; Mørup, S. Identification of green rust in an ochre sludge. *Clay Miner.* **1991**, *26*, 577–582. [CrossRef]

111. Root, R.A.; Dixit, S.; Campbell, K.M.; Jew, A.D.; Hering, J.G.; O'Day, P.A. Arsenic sequestration by sorption processes in high-iron sediments. *Geochim. Cosmochim. Acta* **2007**, *71*, 5782–5803. [CrossRef]
112. Trolard, F.; Bourrié, G.; Abdelmoula, M.; Refait, P.; Feder, F. Fougerite, a new mineral of the pyroaurite-iowaite group: Description and crystal structure. *Clays Clay Miner.* **2007**, *55*, 323–334. [CrossRef]
113. Mills, S.J.; Christy, A.G.; Génin, J.M.R.; Kameda, T.; Colombo, F. Nomenclature of the hydrotalcite supergroup: Natural layered double hydroxides. *Mineral. Mag.* **2012**, *76*, 1289–1336. [CrossRef]
114. Génin, J.M.R.; Mills, S.J.; Christy, A.G.; Guérin, O.; Herbillon, A.J.; Kuzmann, E.; Ona-Nguema, G.; Ruby, C.; Upadhyay, C. Mössbauerite, $Fe_6^{3+}O_4(OH)_8[CO_3]\cdot 3H_2O$, the fully oxidized 'green rust' mineral from Mont Saint-Michel Bay, France. *Mineral. Mag.* **2014**, *78*, 447–465. [CrossRef]
115. Parmar, N.; Gorby, Y.A.; Beveridge, T.J.; Ferris, F.G. Formation of green rust and immobilization of nickel in response to bacterial reduction of hydrous ferric oxide. *Geomicrobiol. J.* **2001**, *18*, 375–385. [CrossRef]
116. Jorand, F.; Zegeye, A.; Landry, F.; Ruby, C. Reduction of ferric green rust by *Shewanella putrefaciens*. *Lett. Appl. Microbiol.* **2007**, *45*, 515–521. [CrossRef]
117. Hansel, C.M.; Benner, S.G.; Neiss, J.; Dohnalkova, A.; Kukkadapu, R.K.; Fendorf, S. Secondary mineralization pathways induced by dissimilatory iron reduction of ferrihydrite under advective flow. *Geochim. Cosmochim. Acta* **2003**, *67*, 2977–2992. [CrossRef]
118. Borch, T.; Fendorf, S. Phosphate interactions with iron (hydr)oxides: Mineralization pathways and phosphorous retention upon bioreduction. In *Adsorption of Metals by Geomedia II Variables, Mechanisms, and Model Applications*; Barnett, M.O., Kent, D., Eds.; Elsevier: New York, NY, USA, 2008; Volume 7, pp. 321–348.
119. Etique, M.; Jorand, F.P.; Ruby, C. Magnetite as a precursor for green rust through the hydrogenotrophic activity of the iron-reducing bacteria *Shewanella putrefaciens*. *Geobiology* **2016**, *14*, 237–254. [CrossRef]
120. Refait, P.; Drissi, S.H.; Pytkiewicz, J.; Génin, J.-M.R. The anionic species competition in iron aqueous corrosion: Role of various green rust compounds. *Corros. Sci.* **1997**, *39*, 1699–1710. [CrossRef]
121. Dong, H.; Fredrickson, J.K.; Kennedy, D.W.; Zachara, J.M.; Kukkadapu, R.K.; Onstott, T.C. Mineral transformation associated with the microbial reduction of magnetite. *Chem. Geol.* **2000**, *169*, 299–318. [CrossRef]
122. Liu, C.; Kota, S.; Zachara, J.M.; Fredrickson, J.K.; Brinkman, C.K. Kinetic analysis of the bacterial reduction of goethite. *Environ. Sci. Technol.* **2001**, *35*, 2482–2490. [CrossRef] [PubMed]
123. Lovley, D.R.; Roden, E.E.; Phillips, E.J.P.; Woodward, J.C. Enzymatic iron and uranium reduction by sulfate-reducing bacteria. *Mar. Geol.* **1993**, *113*, 41–53. [CrossRef]
124. Hering, J.G.; Stumm, W. Oxidative and reductive dissolution of minerals. In *Mineral-Water Interface Geochemistry*; Hochella, M.F.J., White, A.F., Eds.; American Mineralogical Society: Washington, DC, USA, 1990; Volume 23, pp. 427–465.
125. Heron, G.; Christensen, T.H. Impact of sediment-bound iron on redox buffering in a landfill leachate polluted aquifer (Vejen, Denmark). *Environ. Sci. Technol.* **1995**, *29*, 187–192. [CrossRef] [PubMed]
126. Rügge, K.; Hofstetter, T.B.; Haderlein, S.B.; Bjerg, P.L.; Knudsen, S.; Zraunig, C.; Mosbæk, H.; Christensen, T.H. Characterization of predominant reductants in an anaerobic leachate-contaminated aquifer by nitroaromatic probe compounds. *Environ. Sci. Technol.* **1998**, *32*, 23–31. [CrossRef]
127. Elsner, M.; Schwarzenbach, R.P.; Haderlein, S.B. Reactivity of Fe(II)-bearing minerals toward reductive transformation of organic contaminants. *Environ. Sci. Technol.* **2004**, *38*, 799–807. [CrossRef] [PubMed]
128. Lee, W.; Batchelor, B. Reductive capacity of natural reductants. *Environ. Sci. Technol.* **2003**, *37*, 535–541. [CrossRef]
129. Scheinost, A.C.; Charlet, L. Selenite reduction by mackinawite, magnetite and siderite: XAS characterization of nanosized redox products. *Environ. Sci. Technol.* **2008**, *42*, 1984–1989. [CrossRef]
130. Scheinost, A.C.; Kirsch, R.; Banerjee, D.; Fernandez-Martinez, A.; Zaenker, H.; Funke, H.; Charlet, L. X-ray absorption and photoelectron spectroscopy investigation of selenite reduction by Fe^{II}-bearing minerals. *J. Contam. Hydrol.* **2008**, *102*, 228–245. [CrossRef]
131. O'Loughlin, E.J.; Kelly, S.D.; Kemner, K.M. XAFS investigation of the interactions of U^{VI} with secondary mineralization products from the bioreduction of Fe^{III} oxides. *Environ. Sci. Technol.* **2010**, *44*, 1656–1661. [CrossRef]
132. Bond, D.L.; Fendorf, S. Kinetics and structural constraints of chromate reduction by green rusts. *Environ. Sci. Technol.* **2003**, *37*, 2750–2757. [CrossRef]

133. Christiansen, B.C.; Geckeis, H.; Marquardt, C.M.; Bauer, A.; Römer, J.; Wiss, T.; Schild, D.; Stipp, S.L.S. Neptunyl (NpO_2^+) interaction with green rust, $GR_{Na,SO4}$. *Geochim. Cosmochim. Acta* **2011**, *75*, 1216–1226. [CrossRef]
134. Erbs, M.; Hansen, H.C.B.; Olsen, C.E. Reductive dechlorination of carbon tetrachloride using iron(II) iron(III) hydroxide sulfate (green rust). *Environ. Sci. Technol.* **1999**, *33*, 307–311. [CrossRef]
135. Hansen, H.C.B.; Bender Koch, C.; Nancke-Krogh, H.; Borggaard, O.K.; Sorensen, J. Abiotic nitrate reduction to ammonium: Key role of green rust. *Environ. Sci. Technol.* **1996**, *30*, 2053–2056. [CrossRef]
136. Hansen, H.C.B.; Guldberg, S.; Erbs, M.; Bender Koch, C. Kinetics of nitrate reduction by green rusts—Effects of interlayer anion and Fe(II):Fe(III) ratio. *Appl. Clay Sci.* **2001**, *18*, 81–91. [CrossRef]
137. Heasman, D.M.; Sherman, D.M.; Ragnarsdottir, K.V. The reduction of aqueous Au^{3+} by sulfide minerals and green rust phases. *Am. Mineral.* **2003**, *88*, 725–738. [CrossRef]
138. Kone, T.; Hanna, K.; Abdelmoula, M.; Ruby, C.; Carteret, C. Reductive transformation and mineralization of an azo dye by hydroxysulphate green rust preceding oxidation using H_2O_2 at neutral pH. *Chemoshpere* **2009**, *75*, 212–219. [CrossRef] [PubMed]
139. Larese-Casanova, P.; Scherer, M.M. Abiotic transformation of hexahydro-1,3,5-trinitro-1,3,5-triazine (RDX) by green rusts. *Environ. Sci. Technol.* **2008**, *42*, 3975–3981. [CrossRef]
140. Lee, W.; Batchelor, B. Abiotic reductive dechlorination of chlorinated ethylenes by iron-bearing soil minerals. 2. Green rust. *Environ. Sci. Technol.* **2002**, *36*, 5348–5354. [CrossRef]
141. Legrand, L.; El Figuigui, A.; Mercier, F.; Chausse, A. Reduction of aqueous chromate by Fe(II)/Fe(III) carbonate green rust: Kinetic and mechanistic studies. *Environ. Sci. Technol.* **2004**, *38*, 4587–4595. [CrossRef]
142. Loyaux-Lawniczak, S.; Refait, P.; Lecomte, P.; Ehrhardt, J.-J.; Génin, J.-M.R. The reduction of chromate ions by Fe(II) layered hydroxides. *Hydrol. Earth Syst. Sci.* **1999**, *3*, 593–599. [CrossRef]
143. Mitsunobu, S.; Takahashi, Y.; Sakai, Y. Abiotic reduction of antimony(V) by green rust ($Fe_4(II)Fe_2(III)(OH)_{12}SO_4{\cdot}3H_2O$). *Chemosphere* **2008**, *70*, 942–947. [CrossRef] [PubMed]
144. Myneni, S.C.B.; Tokunaga, T.K.; Brown, G.E., Jr. Abiotic selenium redox transformations in the presence of Fe(II,III) oxides. *Science* **1997**, *278*, 1106–1109. [CrossRef]
145. O'Loughlin, E.J.; Burris, D.R. Reduction of halogenated ethanes by green rust. *Environ. Toxicol. Chem.* **2004**, *23*, 41–48. [CrossRef]
146. O'Loughlin, E.J.; Kelly, S.D.; Csencsits, R.; Cook, R.E.; Kemner, K.M. Reduction of uranium(VI) by mixed iron(II)/iron(III) hydroxide (green rust): Formation of UO_2 nanoparticles. *Environ. Sci. Technol.* **2003**, *37*, 721–727. [CrossRef] [PubMed]
147. O'Loughlin, E.J.; Kelly, S.D.; Kemner, K.M.; Csencsits, R.; Cook, R.E. Reduction of Ag^I, Au^{III}, Cu^{II}, and Hg^{II} by Fe^{II}/Fe^{III} hydroxysulfate green rust. *Chemoshpere* **2003**, *53*, 437–446. [CrossRef]
148. Pepper, S.E.; Bunker, D.J.; Bryan, N.D.; Livens, F.R.; Charnock, J.M.; Pattrick, R.A.D.; Collison, D. Treatment of radioactive wastes: An X-ray adsorption spectroscopy study of the treatment of technetium with green rust. *J. Colloid Interface Sci.* **2003**, *268*, 408–412. [CrossRef]
149. Refait, P.; Simon, L.; Génin, J.-M.R. Reduction of SeO_4^{2-} anions and anoxic formation of iron(II)-iron(III) hydroxy-selenate green rust. *Environ. Sci. Technol.* **2000**, *34*, 819–825. [CrossRef]
150. Skovbjerg, L.L.; Stipp, S.L.S.; Utsunomiya, S.; Ewing, R.C. The mechanisms of reduction of hexavalent chromium by green rust sodium sulphate: Formation of Cr-goethite. *Geochim. Cosmochim. Acta* **2006**, *70*, 3582–3592. [CrossRef]
151. Williams, A.G.B.; Scherer, M.M. Kinetics of Cr(VI) reduction by carbonate green rust. *Environ. Sci. Technol.* **2001**, *35*, 3488–3494. [CrossRef]
152. Yan, S.; Boyanov, M.I.; Mishra, B.; Kemner, K.M.; O'Loughlin, E.J. U(VI) reduction by biogenic and abiotic hydroxycarbonate green rusts: Impacts on U(IV) speciation and stability over time. *Environ. Sci. Technol.* **2018**, *52*, 4601–4609. [CrossRef]
153. Etique, M.; Zegeye, A.; Gregoire, B.; Carteret, C.; Ruby, C. Nitrate reduction by mixed iron(II-III) hydroxycarbonate green rust in the presence of phosphate anions: The key parameters influencing the ammonium selectivity. *Water Res.* **2014**, *62*, 29–39. [CrossRef] [PubMed]